

SOLAR ULTRAVIOLET RADIATION
IN SWEDEN

Weine Josefsson

SOLAR ULTRAVIOLET RADIATION IN SWEDEN

Weine Josefsson

This report is part of the work within a project (SSI P 169-85) supported by the National Institute of Radiation Protection in Stockholm (Statens Strålskyddsinstitut).

Issuing Agency SMHI S-601 76 Norrköping SWEDEN	Report number RMK 53	
Author (s) Weine Josefsson	Report date October 1986	
Title (and Subtitle) SOLAR ULTRAVIOLET RADIATION IN SWEDEN		
Abstract <p>The ultraviolet radiation and the column amount of ozone has been recorded in Norrköping, 58.58 N, 16.15 E, Sweden since 1983. The results made it possible to develop a simple model for computing the average spatial distribution of DUV. The different wavelengths were weighted according to a biological action spectrum and summed to give the DUV. The amount of solar DUV radiation depends strongly on solar altitude. That is clearly seen in the daily and yearly course and in the spatial distribution as a decrease with latitude. The effects of the column amount of ozone, turbidity, altitude, cloudiness and the ground reflectance were included in the model calculations. The UV-spectral irradiance varies strongly with the solar height and the amount of ozone.</p> <p>Especially the effect of ozone is remarkable. It causes a steep decrease of irradiance for shorter wavelengths. The average yearly course of the amount of ozone will shift the average maximum of DUV from the end of June to the mid of July. Usually in Sweden the diffuse DUV solar irradiance is larger than the direct solar component. Therefore the diffuse component alone can cause damage.</p>		
Key words Ultraviolet solar radiation (UV), Ozone, Brewer, Damaging UV, Erythema, Spatial distribution, UV-spectrum		
Supplementary notes The work was financed by SSI	Number of pages 71	Language English
ISSN and title 0347-2116 SMHI Reports Meteorology and Climatology		
Report available from: SMHI S-601 76 Norrköping SWEDEN		

TABLE OF CONTENTS

	TERMINOLOGY AND ABBREVIATIONS	
1	INTRODUCTION	
1.1	Physics of UV-solar radiation	1
1.2	Ozone in the atmosphere	2
1.3	Effects of UV radiation	3
2	METHODS OF MEASUREMENT	
2.1.1	Brewer Ozonespectrophotometer	4
2.1.2	Measurement of ozone and sulphur dioxide	6
2.1.3	Measurement of UVB and DUV	9
2.1.4	Calibration	10
2.2.1	Other instruments used	13
3	DISCUSSION OF THE ACCURACY	
3.1	Accuracy of the Brewer	14
3.2	Accuracy of the other instruments	17
4	FACTORS INFLUENCING THE UV-SOLAR RADIATION	
4.1	Solar height	18
4.2	Ozone	20
4.3	Ground reflectance	21
4.4	Clouds	23
4.5	Turbidity	25
4.6	Altitude	26
5	RESULTS OF THE MEASUREMENTS	
5.1	UVA solar radiation	27
5.2	UVB solar radiation	29
5.3	DUV solar radiation	30
5.4	Erythemal solar radiation	35
5.5	UV spectra	37
5.6	UV sky distribution	40
5.7	Ozone measurements	42
5.8	Sulphur dioxide measurements	43
6	SPATIAL DISTRIBUTION OF DUV	
6.1	Description of the method	44
6.2	Comments on the spatial distribution	47
6.3	Clear day data	49
	ACKNOWLEDGEMENTS	55
	REFERENCES	56
	APPENDIX	58

TERMINOLOGY AND ABBREVIATIONS

- Diffuse Radiation - (a) Solar radiation which is scattered in transmission through the atmosphere
(b) direct and/or diffuse radiation (a) reflected by nonspecular surfaces.
- Direct Radiation - Radiation coming directly from the sun's disk
- D. U. - Dobson Unit approximately equal to milli-atm cm. If a column amount of ozone of 300 D. U. were condensed at the surface of earth, at standard pressure and temperature it would correspond to a layer of pure ozone only 3 mm thick.
- DUV - Damaging Ultra Violet radiation in this report defined as the solar radiation weighted by the ACGIH-NIOSH curve.
- ERY - Erythemally active radiation, in this report defined as the solar radiation weighted by the response curve proposed by Green et al, CIAP 5 (1975).
- Extraterrestrial Radiation - The solar radiation which would be received on a surface if there were no atmosphere.
- Global - Refers to solar radiation as received on earth; sum of direct and diffuse components; applied as global irradiance or global irradiation.
- Irradiance - The rate at which radiant energy is incident on a surface, per unit area of surface (Units: energy/time/area).
- Irradiation - The energy incident on a surface over some specified period of time, per unit area of surface (Units: energy/area).
- Octas - Fraction of the sky covered by clouds, 0 is cloudfree and 8 is overcast
- Radiant energy - Energy in the form of photons or electromagnetic waves.
- Turbidity - Generally smoke, haze and dust which reduces the transmission of radiation in the atmosphere.
- Stratosphere - The atmospheric layer about 8 - 50 km, in the lower stratosphere where the temperature increases due to absorption of solar radiation by ozone.
- UVA - Ultraviolet radiation in the wavelength range 315 to 400 nm.
- UVB - Ultraviolet radiation in the wavelength range 280 to 315 nm.

UVC

- Ultraviolet radiation in the wavelength range 200 to 280 nm.

UNIT CONVERSION

1 Wh = 3 600 J

1 D.U. = 1 milli-atm-cm, STP (Standard Temperature and Pressure)

A column with the base of a square metre of

1 milli-atm-cm SO₂ corresponds to 28.6 mg SO₂

1 milli-atm-cm Ozone corresponds to 21.4 mg Ozone

1 INTRODUCTION

1.1 UV-solar radiation

The distribution of energy in the solar spectrum shows a peak in the visible region and a fast decline in the ultraviolet region, Figure 1.1. Only 8% of the solar output is in the ultraviolet and less than 2% is in the wavelength range of interest, i.e. for erythema. Using the concept of the dual character (wave - particle) of electromagnetic radiation, such as solar radiation, the photon (particle) has an energy that depends only on the inverse of the wavelength. The energy of an ultra-violet photon at 300 nm is twice that of a visible photon at 600 nm.

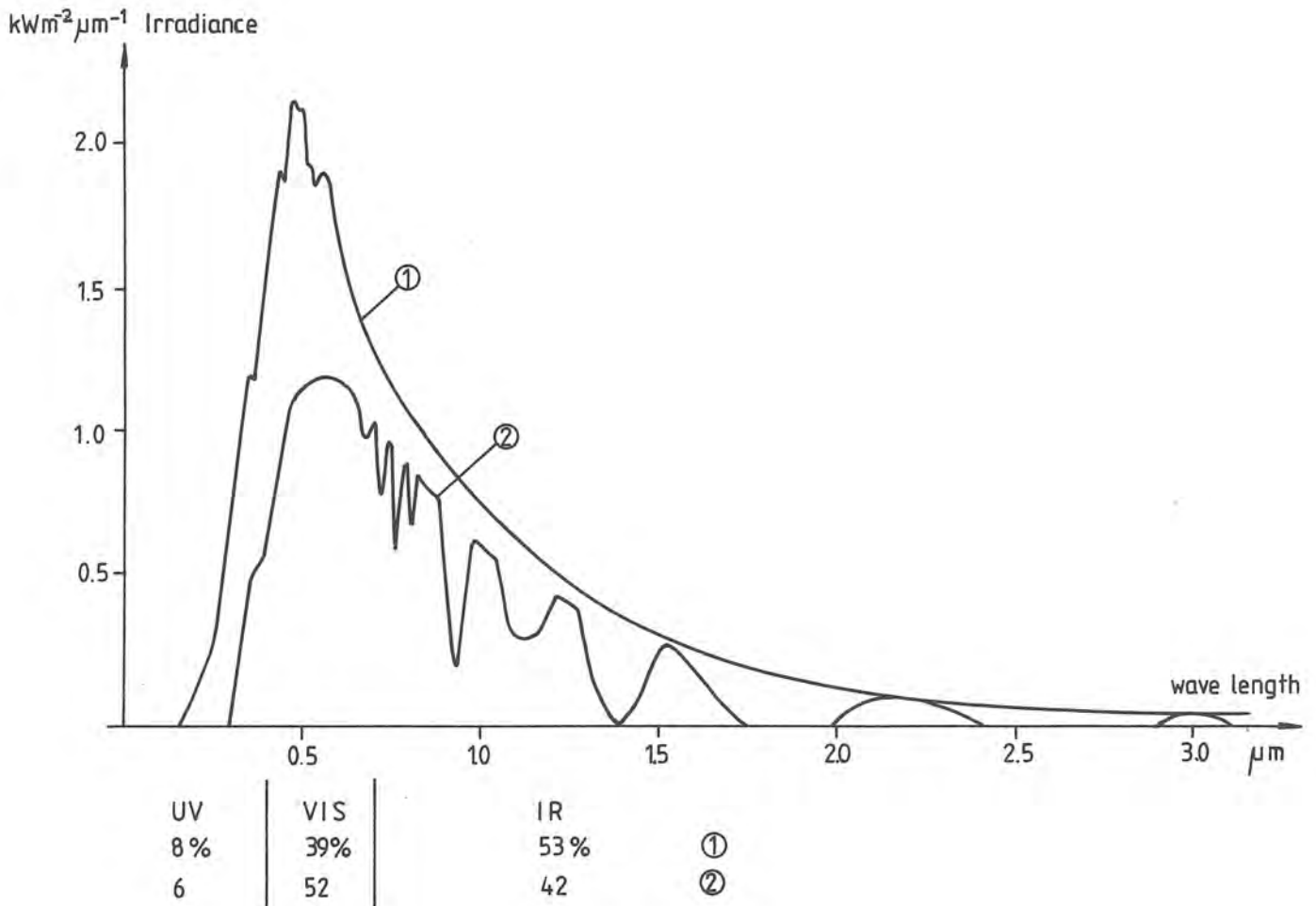


Figure 1.1 The spectral distribution of solar radiation outside the atmosphere, 1, and at sealevel, 2, with a high sun and no clouds. The percentages illustrates the relative distribution within the two spectra.

The UV spectral region is usually divided in three regions UVC (200 - 280 nm), UVB (280 - 315 nm) and UVA (315 - 400 nm). Due to absorption in the upper atmosphere the UVC does not reach the surface of the earth. The absorption by atmospheric gases, mainly ozone is so strong that essentially no solar radiation with wavelengths below 290 nm will penetrate the atmosphere. Above 290 nm the absorption by ozone decreases rapidly as the wavelength increases and the UVA region is virtually unaffected. However, the UVB-region is highly affected by varying content of ozone.

Other important effects are the scattering of radiation by air molecules, aerosols and clouds. It removes radiation from the direct beam and redistributes it as diffuse radiation. The molecular scattering is proportional to the inverse fourth power of the wavelength. Therefore it is much more effective for shorter wavelengths and it is the cause of the colour of the blue sky. The molecular scattering is so much greater in the UV than in the visible that the diffuse UV-radiation is almost always greater than the direct UV-radiation. In summer at noon with a clear sky the diffuse radiation contributes to the global radiation with about 20 - 25 % in the visible, with about 50% in the UVA and about 70% in the UVB. It is important to note that most irradiation values discussed in this report refer to a horizontal surface having a free horizon, i.e. no obstructions.

The scattering by aerosols and clouds is relatively independent of the wavelength. But the wide range of variation in the content of aerosols, often expressed as turbidity, and the variety of different cloud types and cloud amounts make these factors contribute to the overall variation of the ultraviolet radiation in a not always predictable way.

The most important factor affecting the ultraviolet radiation received on a surface is the geometry, i.e. the position of the surface relative the sun, obstructions and nearby reflecting surfaces. For the horizontal surface the solar height determined by the latitude, the day of the year and the time of the day is the primary factor. This can easily be seen in the yearly and daily course with the highest irradiances in the summer and in the hours around noon. The dependence on solar height is more pronounced for the UV-radiation compared to the visible radiation.

1.2 The ozone in the atmosphere

The molecule formed by three atoms of oxygen called ozone plays a key role in the photochemical processes not only in the upper atmosphere but also in the lowest parts of the atmosphere. Measurements of the vertical distribution of ozone show that most of the atmospheric ozone is in the lower stratosphere, 10-30 km above ground, Figure 1.2.

An average value of the total column ozone is around 0.3 cm STP, i.e. a 0.3 cm thick layer of pure ozone at standard temperature (0 C) and pressure (101.325 kPa). This small amount of gas is enough to protect the biosphere from most of the damaging ultraviolet radiation. Any changes of ozone concentrations due to human activities or due to natural causes would result in a change of the UV-radiation absorbed in the stratosphere and consequently in a change of the UV-radiation received at the ground. This will have biological as well as climatological consequences.

Most ozone is formed at upper stratospheric levels as a result of photodissociation of molecular oxygen and a following reaction between atomic and molecular oxygen. A balance between forming and destruction of ozone

is achieved through catalytic reactions involving e.g. HO^{\cdot} , NO^{\cdot} and ClO and through the recombination between atomic oxygen and ozone. Because of the low reaction rate coefficient of some reactions the circulation in the stratosphere is of major importance for the distribution of ozone in the atmosphere.

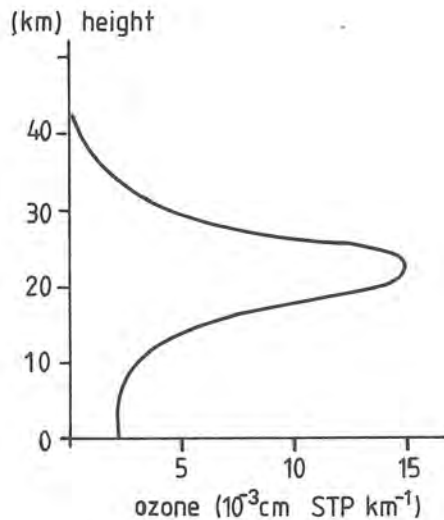


Figure 1.2 A typical smoothed vertical distribution of ozone.

1.3 Effects of the UV-radiation

As mentioned the UV-photons inherits a high potential energy able to cause damaging effects on materials and on living cells. Well known are the degradation of paints, polymers and the causation of erythema and photokeratitis. There are also positive effects such as killing germs and synthesizing of vitamin D. The fundamental process of these effects is the absorption of a photon by a molecule changing or destroying the molecule. The sensitivity to UV-radiation, e.g. the erythema effect on skin, varies with wavelength depending on the energy of the photons and the required energy for the reaction and depends of course of the type of skin.

There exists several curves describing the relative spectral effectiveness upon the skin and the eyes. In this report a curve proposed by ACGIH (Sloney, 1972) have been used. It is an envelope curve for several threshold data, erythema, photokeratitis etc. The result is recorded as DUV, Damaging UltraViolet radiation; See section 2.1.3.

2 METHODS OF MEASUREMENT

2.1.1 Brewer ozone spectrophotometer

The Brewer instrument used for the measurement of the atmospheric column amount of ozone is designed and built in Canada.

The instrument has the dimensions 70 x46 x21 cm. It is mounted on a small box containing the azimuth drive. The Brewer instrument is connected to 220 V, AC and to a pet computer. The box is weatherproof and it is also protected against overvoltages caused by lightning. Measurements of the global radiation is taken through a plastic diffusor shielded by a dome of quartz and the direct sun and the zenith sky is observed through a slant quartz window. An observing window on the top of the Brewer gives the opportunity to check if the proper adjustments are made for each type of observation. The software of the computer controls the dataflow between the computer and the Brewer as well as it makes it possible to move any of the six stepping motors or to check the status of the photo-

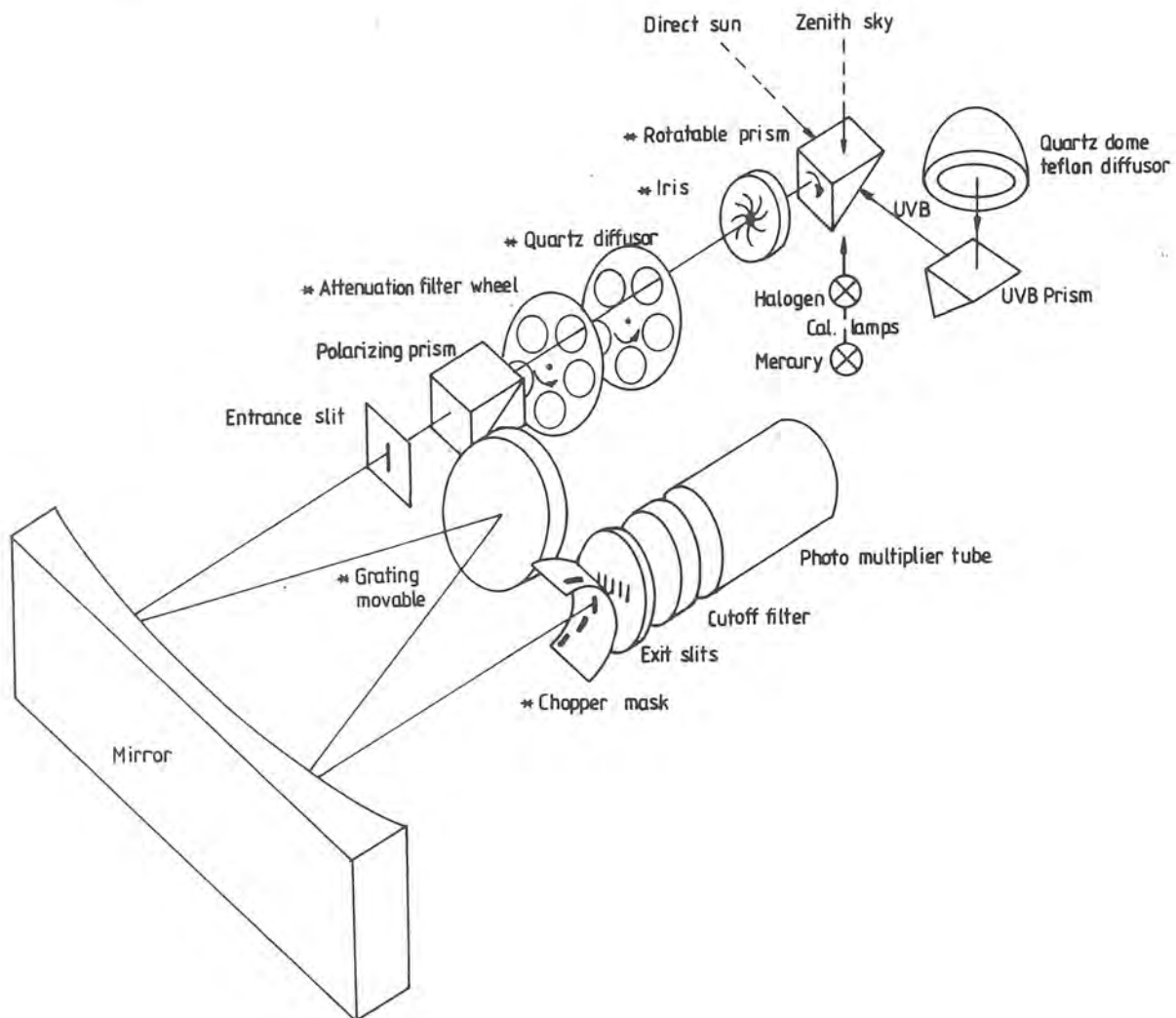


Figure 2.1 Schematic top view of the optical system of Brewer No 6, all lenses are omitted. A star indicate connection with a stepping motor.

The essential features of the optical system of the Brewer is illustrated in Figure 2.1. An adjustable prism can be set in alternative positions. If directed downwards it sees either a mercury lamp (wavelength cal.) or a halogen lamp (irradiance standard) and directed backwards it is able to observe the diffused light from sun and sky through a "lightshaft". In the upward position it sees the zenith sky and adjusted according to the actual solar zenith angle it is possible to observe the direct radiation from the sun. The azimuth drive ensures that the Brewer always points correctly in the azimuthal direction of the sun.

The light from the prism passes through an iris and an attenuation filter and is in some cases diffused by a quartz plate. A quartz lens collimates the light along the optical axis and it is positioned such that its focus is at the plane of the iris. After passing a polarizer and the entrance slit the light is reflected by a mirror to the grating. The second order spectrum is after reflection of the mirror focused on the plane of the exit slits. A movable chopper mask exposes one slit a time. Behind the slits a cut-off filter ensures that no visible light enters the photomultiplier. Most of the functions are connected with stepping motors which are controlled by the computer. The iris, for instance, is usually set in two different positions, open or closed. The closed position, a small opening approximately three solar diameters, is used to shade the unwanted sky radiation when observing the direct sun. The intensity of the ultraviolet radiation spans over several orders of magnitude but the radiation entering the photomultiplier is adjusted to its range of measurement by inserting an appropriate attenuation filter.

The polarizing filter reduces the difference between the clear sky and the cloudy sky measurements due to the clear sky's strongly polarized Rayleigh scattered radiation.

The movable grating is connected with a stepping motor via a micrometer. This makes it possible to scan the spectrum. One step of the motor corresponds to approximately 0.007 nm change in the spectrum on the exit slits.

The exit slits are fixed in their positions in front of the photomultiplier. Table 2.1 gives the wavelengths of the slits when the grating is in the position for an ozone observation. The movable chopping mask makes it possible to expose only one slit and to make series of measurements.

NR	WAVELENGTH (nm)	RESOLUTION BASE WIDTH (nm)	OZONE ABS (cm ⁻¹ , base e)
1	306.296	1.052	4.1163
2	310.048	1.041	2.3139
3	313.510	1.066	1.5553
4	316.808	1.053	0.8659
5	320.012	1.018	0.6861
	302.2	mercury calibration	

Table 2.1 Data from J. Kerr who tested Brewer Nr 6 in Oct 1983. Slits Nr 2 and 4 are also used for linearity tests.

2.1.2 Measurements of ozone and sulphurdioxide

Counts, N_i , are read in from the Brewer from the combination of slits chosen (1 - 5). The dark counts, N_d , are subtracted and the remaining counts are converted to count rate (taken into account the number of cycles, C_y , the time per cycle and the dark interval between each slit reading, IT).

$$N = (N_i - N_d) * 2 / C_y / IT \quad (2-1)$$

The dead time of the photon counting system is compensated. Poisson statistics are assumed so that for any observation at true count rate N_0 (counts/s) the observed rate N will be

$$N = N_0 * \exp(-N_0 * t_d) \quad (2-2)$$

where, t_d , is the dead time (seconds). The equation is solved by iteration to get N_0 from N .

To allow integer arithmetic $10 \log(N_0)$ is taken for each count and the result is scaled by 10000 .

$$N_0 = 10000 * 10 \log(N_0) \quad (2-3)$$

This value is corrected for the temperature in the band pass filter and for the attenuation of the filter wheel.

$$N_c = N_0 + T_c + AF \quad (2-4)$$

If the reading is on the direct sun the count is adjusted by compensating the effect of Rayleigh scattering for the airmass calculated for the time of the observation.

The measured intensity of direct sunlight at each wavelength, i , is given by

$$N_c(i) = N_{ex}(i) - S_r(i) * m_1 - S_d(i) * \sec ZA - a_0(i) * 0.3 * m_3 - a_s(i) * S_{O_2} * m_2 \quad (2-5)$$

where

$N_c(i)$	is the $10 \log$ of the measured intensity, at wavelength i , scaled by 10000
$N_{ex}(i)$	is the $10 \log$ of the extraterrestrial intensity at wavelength i , scaled by 10000
$S_r(i)$	is the Rayleigh scattering coefficient, at wavelength i , scaled by 10000
m_1	is the optical airmass for the direct sunlight
$S_d(i)$	is the aerosol scattering coefficient, at wavelength i , scaled by 10000
$\sec ZA$	is the secant of the solar zenith angle

$a_0(i)$	is the ozone absorption coefficient, at wavelength i , scaled by 10000
O_3	is the column amount of ozone
m_3	is the optical path length through the ozone layer
$a_S(i)$	is the SO_2 absorption coefficient, at wavelength i , scaled by 10000
SO_2	is the column amount of sulphur dioxide
m_2	is the optical path length through the sulphur dioxide

The equation above and the intensity measurements for the Brewer wavelengths 2 to 5 can be combined to the following expression

$$M = M_0 - D_r * m_1 - D_d * \sec ZA - D_{a0} * O_3 * m_3 - D_{aS} * SO_2 * m_2 \quad (2-6)$$

where

$$\begin{aligned} M &= N_c(2) - 0.5 * N_c(3) - 2.2 * N_c(4) + 1.7 * N_c(5) \\ M_0 &= N_x(2) - 0.5 * N_x(3) - 2.2 * N_x(4) + 1.7 * N_x(5) \\ D_r &= S_r(2) - 0.5 * S_r(3) - 2.2 * S_r(4) + 1.7 * S_r(5) \\ D_d &= S_d(2) - 0.5 * S_d(3) - 2.2 * S_d(4) + 1.7 * S_d(5) \\ D_{a0} &= a_0(2) - 0.5 * a_0(3) - 2.2 * a_0(4) + 1.7 * a_0(5) \\ D_{aS} &= a_S(2) - 0.5 * a_S(3) - 2.2 * a_S(4) + 1.7 * a_S(5) \end{aligned}$$

The coefficients 1, -0.5, -2.2 and 1.7 have been selected to give a negligible value of D_d and it also gives a negligible value of D_{aS} . This is possible if S_d is a slowly varying monotonic function of wavelength. Ignoring the negligible terms of the expression above it can be rewritten to give the column amount of ozone as

$$O_3 = (M_0 - M - D_r * m_1) / (D_{a0} * m_3) \quad (2-7)$$

All the parameters required to solve the equation can be determined. M is measured, m_1 and m_3 are calculated, D_r is calculated from scattering theory and D_{a0} is known from laboratory measurements. The term M_0 could be determined by measurements outside the atmosphere or experimentally by linear extrapolation, equation (2-6), if the assumption that the attenuation parameters remain constant during the experiment. However, in practice this assumption is not fulfilled and such determinations of M_0 are often unreliable. Besides there are factors depending on the design and adjustment of the Brewer that affect the spectral responsivity of the instrument. The extraterrestrial values are usually determined by direct intercomparison of the instrument against one well-calibrated reference instrument. Therefore the extraterrestrial values will include instrument dependent factors and will vary between different instruments. There is also a risk of variation with time due to the continuous outdoor exposition of the instrument.

The column amount of sulphur dioxide is given by combining the intensity measurements from the Brewer wavelengths 1, 4 and 5 as

$$S = S_{ex} - D_{Sr} * m_1 - D_{Sa0} * 0.03 * m_3 - D_{SaS} * S_{O2} * m_2 \quad (2-8)$$

where

$$S = N_c(1) - 4.2 * N_c(4) + 3.2 * N_c(5)$$

$$S_{ex} = N_{ex}(1) - 4.2 * N_{ex}(4) + 3.2 * N_{ex}(5)$$

$$D_{Sr} = S_r(1) - 4.2 * S_r(4) + 3.2 * S_r(5)$$

$$D_{Sa0} = a_0(1) - 4.2 * a_0(4) + 3.2 * a_0(5)$$

$$D_{SaS} = a_S(1) - 4.2 * a_S(4) + 3.2 * a_S(5)$$

The different terms in the expression above can be determined in a similar way as for the ozone equation. The column amount of SO₂ is given by

$$S_{O2} = \frac{(S_{ex} - S - D_{Sr} * m_1 - D_{Sa0} * 0.03 * m_3)}{(D_{SaS} * m_2)} \quad (2-9)$$

2.1.3 Measurement of UVB and DUV

The UV-radiation falling on the horizontal teflon diffusor of the instrument is directed into the optics by a field prism and by the rotatable prism, see Figure 2.1.

The iris is open, the quartz diffusor is out and there is no attenuation filter. Only one slit is used and by moving the grating it is possible to scan the spectrum.

A scan starts at 290 nm and proceeds normally to 320 nm (before 4 Sep, 1984 to 315 nm) and then back to 290 nm by a step-length of 0.5 nm. Other values of the step-length are optional. This loop will go on until the measurements are stopped. In this case the grating is positioned in the calibrated position, to make ozone measurements possible.

The lower limit of the wavelength range is chosen to be at a shorter wavelength than the lower boundary of the ultraviolet solar spectrum at the surface of earth. Almost no radiation is observed below 295 nm. The upper limit was chosen to coincide with the definition of the UVB (280-315 nm). However, to make it possible to compute the erythemal dose (ERY) given by a response curve proposed by Green et al, CIAP (1975), the upper limit was set to 320 nm. The values measured at each wavelength are corrected for the number of cycles, dead time, temperature etc; see section 2.1.2.

The absolute irradiance is computed by using a calibration function. Integration of the UVB and the computation of DUV and ERY is straight forward. The response curves used can be analytically expressed as

$$R_{DUV}(w) = 0.3 * 0.74^{(w-300)} \quad \text{if } w > 300 \quad (2-10)$$

$$R_{DUV}(w) = 1.0 - 0.36 * ((w-270)/20)^{1.64} \quad \text{if } w \leq 300 \quad (2-10)$$

and

$$R_{ERY}(w) = (4 * \exp((w-297)/3.21)) / ((1 + \exp((w-297)/3.21))) \quad (2-11)$$

Equations (2-9) based on data from Sliney (1972) are given by Wester (1981) and equation (2-10) is given by Green et al, CIAP 5 (1975). The solar irradiance, $I(w)$, is weighted for each measured wavelength, w , by the response function $R(w)$ and the DUV is calculated as

$$DUV = 0.5 * \int_{290}^{315} R(w) * I(w) * dw + \sum_{w=290}^{315} R(w) * I(w) * \Delta w \quad (2-12)$$

The measurements taken at the boundaries, 290 and 315 nm, are treated as if half of the radiation is in the range of interest. This assumption is not critical because at 290 nm the irradiance is zero at the surface of earth and at 315 nm is the response function $R(w)$ very small.

2.1.4 Calibration

The first absolute calibration was performed at the National Institute of Radiation Protection (SSI) on the 22nd of February 1983. Two different lamps were used as irradiance sources. (General Electric DXW 1000-W). The lamps have been calibrated at the "Swedish Testing Institute" in Borås, SP, at different wavelengths in steps of 10 nm. The data are therefore traceable to the National Bureau of Standards, U S A. Values for each wavelength were achieved by interpolation between the calibrated points assuming "black body radiation". The lamp was mounted 0.50 m above the diffusor. After a warm up of the lamp a scan of the spectral range 290 - 315 was done. The current through the lamp was controlled and stabilized to 8.000 A. The counts for each wavelength were recorded and a smoothed calibration function was computed.

$$K(w) = -1204.8 + 6.98*w \quad \text{for } 290 \leq w < 310 \text{ nm}$$

$$K(w) = 236125 - 1527.4*w + 2.45*w*w \quad \text{for } 310 \leq w \leq 315 \text{ nm}$$

where w is the wavelength in nm and the unit of $K(w)$ is $nW/m^2/nm/pulse$.

According to SP the inaccuracy of the lamp is 5% in the ultraviolet part of the spectrum. The average scatter of the measurements around the smoothed calibration curve is about 2 - 3%. As the wavelength range was extended from 315 nm to 320 nm the calibration function was extrapolated to 320 nm. This was done to make it possible to compare the weighted irradiation computed from the ACGIH-NIOSH curve with that proposed by Green et al (CIAP5, 1975).

The number of counts was of the order of 2000 - 4000 in the 290 - 315 nm range. At real conditions the number of counts is less than 1000 for wavelengths less than 300 nm. For longer wavelengths the number of counts can be anything between 0 and 200 000, but the assumption of linearity in this large range is plausible.

The second absolute calibration was performed on the 20th of June, 1984. The same lamp was used. The result pointed on an increase of the sensitivity of the instrument by approximately 10%. However examining the data it was discovered that the calibration was disturbed by the UV light from a fluorescent lamp in the roof. A reconstruction of the situation made it possible to make a rough correction of the influence from the fluorescent lamp, resulting in correspondence with the previous calibration, within 5%. Therefore the used calibration function was not changed. At the same day it was possible to make simultaneous measurements with the Brewer Nr 6 and an Optronic Mod. 742 spectroradiometer. Data is presented in Figure 2.2. Unfortunately, the cloudcover was broken and the irradiance varied a lot. Despite this and different methods and times used to measure the UVB the correlation is striking. This strengthened the assumption that the Brewer responsivity had not changed much since the first absolute calibration.

A third absolute calibration was performed on the 28th of November 1984. This time another lamp was borrowed from SSI. With the simple equipment that was used it was not possible to adjust the current finely enough. By making several measurements with slightly different currents it was possible to show that the measured irradiance was within 10% of the specified output of the lamp. The wavelength range of the calibration was now extended to 320 nm.

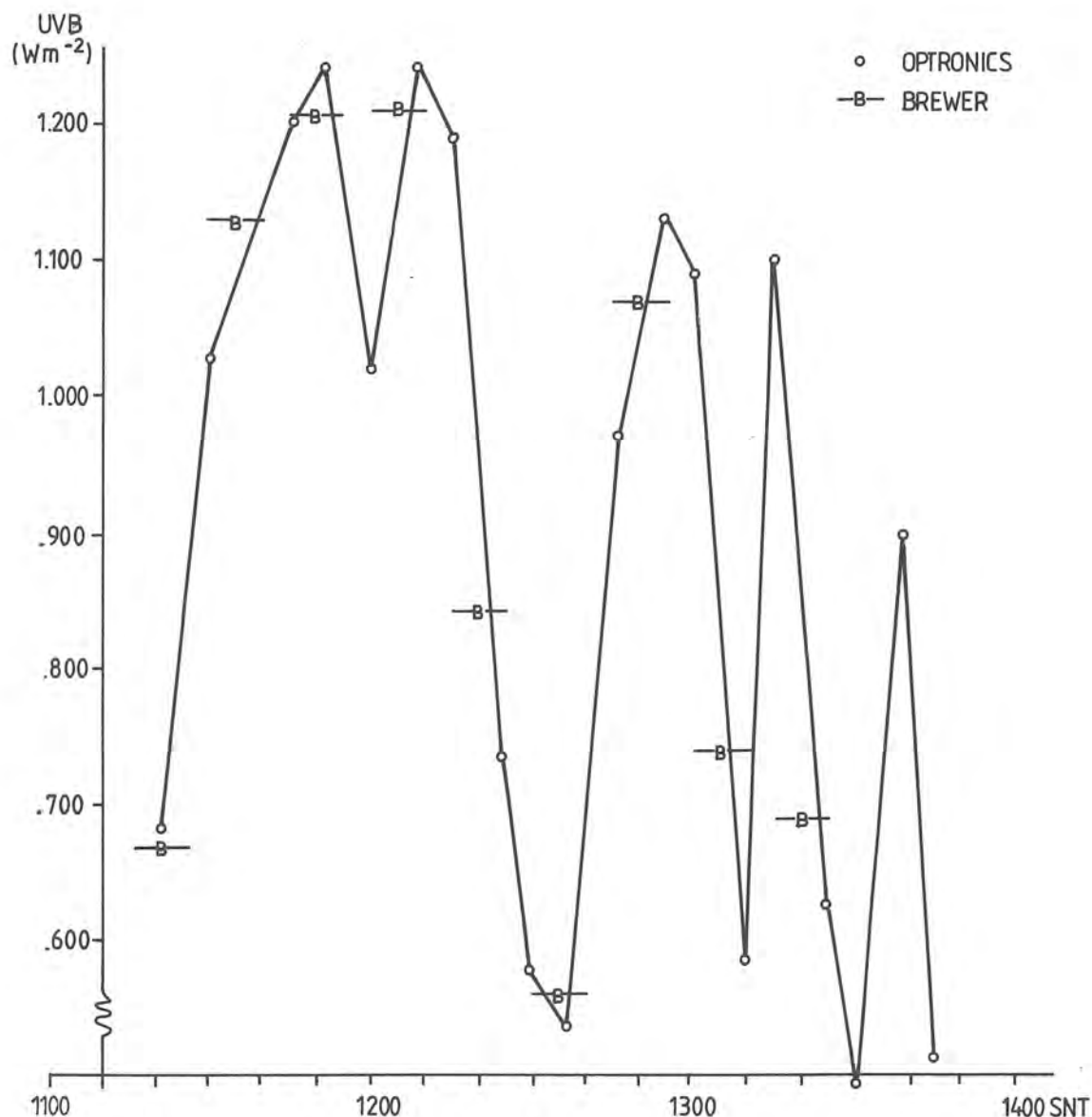


Figure 2.2 Parallel measurements with the Brewer and an Optronic Mod.742 spectroradiometer on the 20th of June 1984.

Conclusion

These calibrations have proved that the sensitivity of the Brewer, used as UVB-spectroradiometer, has been unchanged within an uncertainty of 10%.

The Brewer is only calibrated for normal incidence, i.e. the deviation from true cosine response was not evaluated in these calibrations. The angular dependance was tested with a projector lamp as radiation source. The test and the results are discussed in section 3.1.

An intercomparison of the Brewer No 6 versus Brewer No 8 at AES in Toronto 28 - 30 September 1983 revealed a mean bias error of the measured total column amount of ozone of -0.1 D.U. with a standard deviation of 1.5 D.U. The corresponding values for the sulphur dioxide was 0.0 and 0.3 matm.cm .

To ensure a good operation of the Brewer there have been tests done more or less frequently. A brief presentation is given below. More details can be found in the Brewer manual available from SCI-TEC. Almost every weekday the wavelength setting has been checked by performing a mercury wavelength calibration. After a five minute warm up of the mercury lamp a wavelength scan of the 302.1 nm mercury line is carried out. The measured values are correlated against a standard wavelength scan. If needed the micrometer connected to the grating is shifted to a new position. The calibration is repeated until two consecutive calibrations agree. Normally the micrometer setting will be within one motor step from the previous position.

The standard lamp test is carried out once a month and also in connection with other tests (except the mercury lamp test). After a five minutes warming up of the lamp seven measurements are made. A calculation analogous to the one made for ozone and SO₂ is performed and recorded. A summary is printed indicating the means and the standard deviations. The summary is logged together with the temperature and number of counts of the fifth wavelength. The first numbers can be used to check the internal stability of the ozone observations and the last ones can be used to check the output of the lamp or the absolute sensitivity of the system.

The Brewer is permanently operated outdoors, but it is sometimes brought indoors for special tests and replacement of desiccants. There are for instance some voltages to be monitored and checked to control the stability of the current to the standard lamp. The operation of the shutter mask motor have to be controlled by performing a shutter run and stop test. Measurement are made with the motor stopped in each position and they are compared to measurements made with the motor running.

2.2.1 Other instruments used

Two other radiometers have been used. One was sited in Luleå (65.5 N, 22.1 E) and the other in Norrköping (58.6 N, 16.2 E) close to the Brewer.

The ultraviolet irradiance is measured in two narrow spectral bands, one in the UVA at 360 nm and the other in the UVB at 306 nm. The receiving surface is a teflon diffusor. A filter stack is positioned above a photodiode, used as the detector. The instrument is constructed and described by Wester (1983).

Wester has shown that the UVA irradiance (315-400 nm) is approximately proportional to the irradiance in a narrow spectral band at 360 nm and that the DUV irradiance is roughly proportional to the irradiance in a narrow spectral band at 306 nm. Assuming this the instrument can be used to record UVA and DUV.

The instruments are primarily calibrated against an Optronic Model 742 spectroradiometer, which is calibrated against the standard lamp, mentioned in section 2.1.4, traceable to a standard from the National Bureau of Standards, U S A. During the period of measurement the instrument in Norrköping have been compared to the DUV-data from the Brewer.

There are also two other types of measurements involved in the project, namely the measurement of 'sunburning units' with the radiometer of Robertson-Berger (Berger, 1976) and the photochemical degradation of polymers (PVC and PPO).

The first measurement is performed with an instrument similar to Wester's instrument. The spectral response of the instrument however resembles the skin's erythema action spectrum. The output is given as counts, which is only a relative measure. By comparison with a reference instrument the instrument is calibrated and the counts can be transformed to 'sunburning units', defined as equal to a minimal erythema dose assuming average untanned Caucasian skin. There are about 25 of these instruments operating in the world, mainly in the U S A. This will make it possible to compare different parts of the world regarding the erythema effects of the solar radiation.

The second method of measurement mentioned above is a part of a cooperative work with "The Institute for Building Research" (SIB) in Gävle, Sweden. Thin films of PVC and PPO are exposed during a month and the degradation is correlated to the measured UV values (Lala, 1984). The goal is to see if there is a significant correlation. The advantage with this method is its simplicity and the low cost, which will make it possible to measure at several sites. One problem is that many films have been destroyed by heavy rain or hard winds.

3 DISCUSSION OF THE ACCURACY

3.1 Accuracy of the Brewer

This section is a brief discussion of a number of parameters affecting the accuracy of solar spectral irradiance measurements with the Brewer instrument. More details on the topic of optical radiation measurements with spectroradiometers can be found in NBS Technical Notes and for example Nicodemus (1981) and Liedquist and Werner (1983).

The large increase of solar irradiance with wavelength in the UV-region points on the necessity of high accuracy in the setting of wavelength. The manufacturer claims that the calibration procedure is capable of measuring the wavelength setting to within 0.003 nm over a temperature range of -20°C to $+40^{\circ}\text{C}$.

One limitation of the wavelength-setting of the Brewer is the stepping motor drive of the grating. The use of indivisible motor-steps gives an error of approximately 0.0035 nm, which is equivalent to one half of a motor-step. The precision in the measurement will be of this magnitude over the operating wavelength and temperature range. However, the relation between motor-steps and wavelength, based on a calibration against the line spectra of a mercury and a cadmium lamp and the everyday made internal wavelength set calibration, will add up to an estimated inaccuracy less than 0.02 nm. The change of the solar irradiance is about 1.5% per 0.02 nm at 300 nm and about 0.75% per 0.02 nm at 310 nm.

Due to the non-linearity of solar spectral irradiance and due to the fact that the measurement for each setting of the slit is made not for a single wavelength but for a wavelength band an error will be introduced. The bandpass of the used slits is 0.6 nm. The magnitude of the error is around 1%. (Saunders and Koskowski, 1978).

The UVB solar spectral irradiance at the Earth's surface covers five orders of magnitude. Therefore the spectroradiometer must have a known responsivity covering this entire range.

The response of the Brewer is assumed to be a linear function of the spectral irradiance. To a certain degree the linearity can be checked. On the chopper mask there is a position, with a double slit, making it possible to expose the exit slits 310.0 and 316.8 nm at the same time. The sum of the outputs from the single slit readings can be compared to the double slit readings.

A well designed and properly used instrument should not produce a non-linearity error of more than a few percent (Saunders and Koskowski, 1978).

The solar radiation is scattered by the earth's atmosphere and is therefore polarized. The degree of polarization is highly variable over the sky and during a day. Therefore it is desirable to have an instrument which is insensitive to polarization. The Brewer, however, might be influenced by the polarization due to the polarizing prism used in the foreoptics. The effect is probably reduced by the use of the teflon diffuser.

The solar radiation arrives at the receiving surface of the Brewer from different directions. A simple test show that the response of the instrument depends on the angle of incidence of the radiation. This is often referred to as azimuth- and cosine- error. Ideally the response is proportional to the cosine of the zenith angle of the incident radiation and it is constant at all azimuth angles.

The tests of the dependences on the direction of incident UV-radiation was carried out indoors.

The equipment used for this test was a projector lamp. By changing the angle of incidence at constant distance between the lamp and the receiving surface (teflon diffusor) the cosine response was tested. The main problems with this simple method was that the lamp was not supplied from a stabilized power source, the beam was not collimated and the irradiance level was low. However, the average value of several measurements was estimated to be within 5 % of a "stable" value.

The azimuth response was tested by rotating the Brewer around the normal of the receiving surface and having the lamp in a fixed position. Any azimuth dependence was not possible to detect. If there is any dependence it is less than 5% which is the estimated accuracy of this simple test.

The deviation from the ideal cosine response was significant and it is presented in Figure 3.1.

The conclusion must be that the measured deviation from the ideal cosine response will give too low recorded values, 10-15% by estimation. It should be noted that no values given in this report have been corrected for this "cosine error".

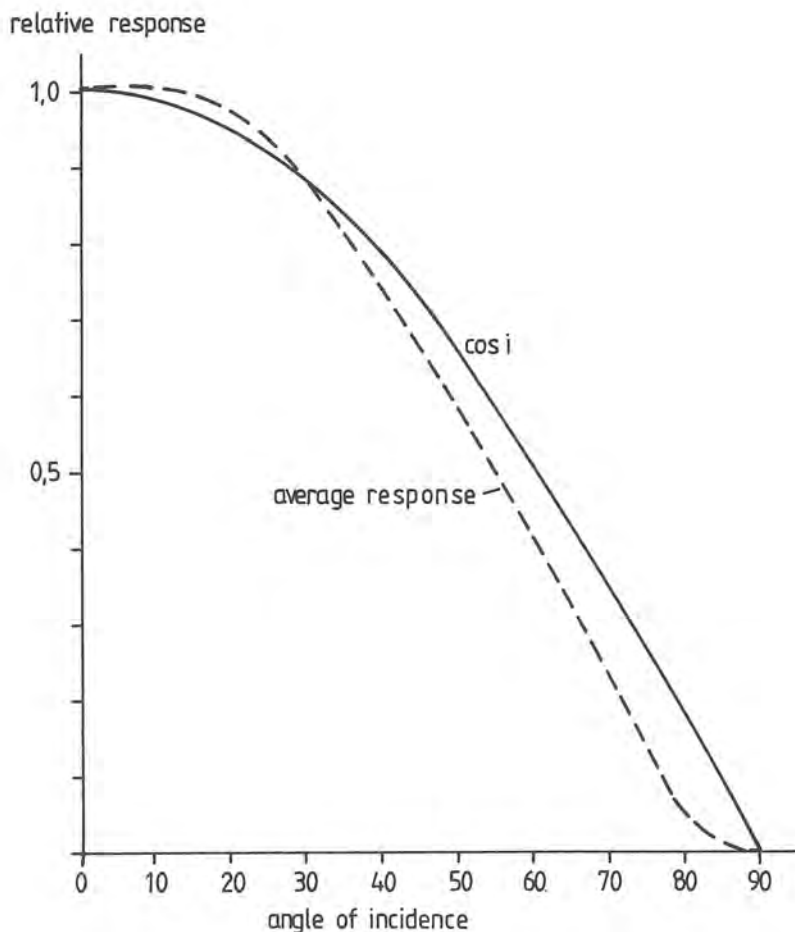


Figure 3.1 Deviation from ideal cosine response for Brewer No 6

Due to the fact that the slit not only transmit a specific band of wavelengths proportional to the width of the slit, but also sees wavelengths far away from the wavelength setting of the instrument an error in the measurements is introduced. The observed solar spectral irradiance will be higher than the true spectral irradiance especially at shorter wavelengths, because of the rapid increase of irradiance with wavelength at this part of spectrum.

Spectral measurements below 300 nm are ambiguous because of the rapid decrease of irradiance with wavelength, the increased relative scattering, and the low signal to noise ratio. This noise is combination of photomultiplier noise and scattered light from longer wavelengths. The noise of the photomultiplier, depending on the temperature, is of the order 10^{-4} to $10^{-5} \text{ Wm}^{-2}\text{nm}^{-1}$.

The temperature dependence have been tested in Canada for each "slit wavelength" used in the ozone observations. This test have been used to establish a linear relation that can be used to correct the UV-measurements at each wavelength. The main temperature dependence is in the cutoff filter in front of the photomultiplier.

The absolute calibration procedure was described in chapter 2.1.4. The spectral irradiance standard used, a halogen lamp, has an uncertainty of approximately 5% in the UVB-region. It has not been possible to make absolute calibrations more frequently than once a year. Therefore the stability of the measurement system is not known well enough.

The procedure used to measure the spectrum introduces some uncertainties in the records. This is because the solar irradiance changes during the spectral scan. To reduce this error the spectrum is scanned from the short end to the long and then back again. The mean value is recorded and the spectrum is related to the time of the turning-point. This procedure is correct if the irradiance is constant or if it is changing linearly during the time of the scan. Individual spectra are well defined for clear skies and uniform cloud-covers, but not for rapidly changing conditions.

Hourly and daily values of DUV and UVB are based on the sums of integrated spectra measured during the hour and during the day. This will cause an error in the individual hourly values, because the measured spectra are not equally distributed during the hour and not frequent enough to describe the variation of the irradiance. However, over a long period the average values will be acceptable. This problem could partly be solved by speeding up the scan by measuring at fewer wavelengths and by averaging the hour values by taking the time of each spectrum into account. Unfortunately a lot of information will be lost if fewer wavelengths are measured. A more advanced method of computing hourly averages has been tested but the software did not work properly.

The rapid change of the UV-irradiance with the solar altitude and consequently with the time points to the importance of a accurate clock in the system. The clock in the computer is not very stable, but correction by the software and by manual checking has minimized the time error to within one minute.

3.2 Accuracy of the other instruments

A discussion of the errors influencing the instruments designed by Wester can be found in the report of Wester (1983). However, the probable cause of the discrepancy between the Brewer and the Wester DUV-values as presented in Table 5.4 and 5.5 will be noted in this section. The values coincide during winter but show large differences during summer (20-30%). By an appropriate change of one or the other instrument constant it is possible to make the values interfere with each other at a suitable time of the year. The discrepancy will remain but removed. One explanation could be that the measurement in a narrow wavelength band around 306 nm does not describe the DUV correctly. Studying some DUV-spectra show that the maximum DUV irradiance at high solar altitudes and low column amounts of ozone is positioned at shorter wavelengths than at low solar altitudes and high column amounts of ozone. Therefore the discrepancy will be varying seasonally as well as daily.

4 FACTORS INFLUENCING THE UV SOLAR RADIATION

The UVB radiation emitted by the sun is approximately constant. The variability is probably less than one percent, see Heath and Thekarakara (1977). This variation is undetectable with measurements at the earth's surface because of the complex influence by atmospheric constituents.

The measured variation can be explained by changing conditions in the atmosphere and in variations of the instrument during the time of measurement. The precision and stability of the instrument is not perfect. Another important factor is the ground albedo.

4.1 Solar height

The most important factor affecting the DUV-irradiance on a horizontal surface is the solar height. To establish a relation between DUV and solar height data from clear days with known column amount of ozone and turbidity were selected. The measured DUV-values were plotted versus the solar height. A relation was established for a column amount of ozone equal to 350 D.U. (See chapter 6.1). The relation was tested and plotted for more extensive data set of hourly values; Figure 4.1 shows the result. The scatter is mainly caused by the inexact method of integrating the hourly values from the individually recorded spectra. Of course the scatter is also depending of variations in the atmosphere, e.g. for each day only one value of the amount of ozone and one value of the turbidity are used. Usually these values are determined around noon. There are days with more or less clouds in the sky. The hours affected by clouds will drop out below the standard curve.

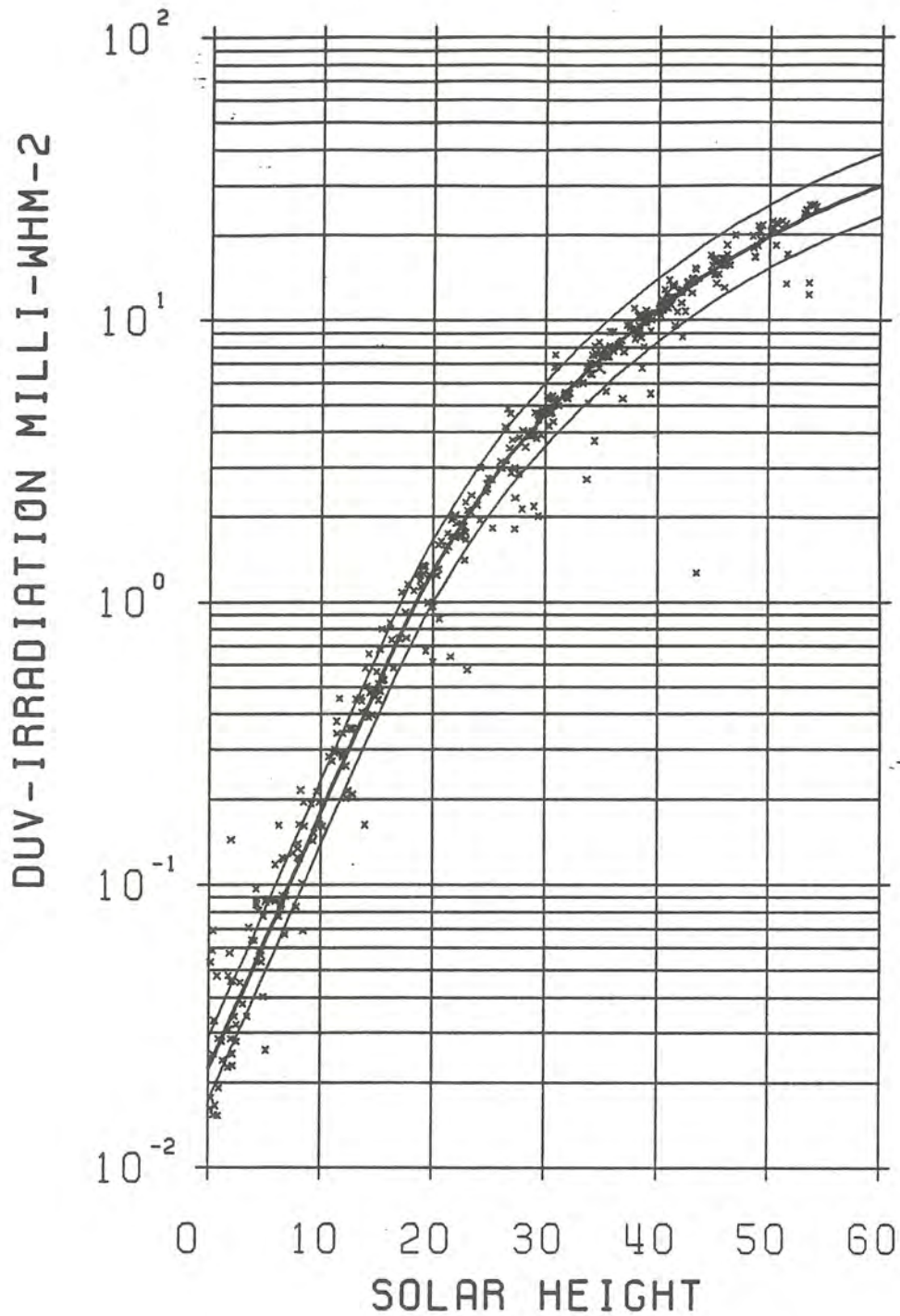


Figure 4.1 Hourly DUV-values versus solar height for "clear days" are plotted as x. The values are normalized to a column amount of ozone of 350 D.U. and an Ångström turbidity coefficient of 0.05. All hours are not cloudfree and there is also a variation in the column amount of ozone and in the turbidity that is not taken into account. The thick full line corresponds to the equations 6-4 a-b valid for 350 D.U., the thin upper line corresponds to 300 D.U. and the thin lower line to 400 D.U.

4.2 Ozone

The effect of ozone on DUV was studied by plotting relative values of DUV for clear days and for the solar heights of 10, 20, 30 and 40 degrees. The data were related to the values of 350 D.U. to find a simple and useful relation. An exponential function as given in chapter 6 was fit to the data. As can be seen in the figure an increase of ozone does not affect the DUV as much as a decrease. In the normal range of variation of ozone the effect will be to half or to double the DUV relative to the DUV-value at 350 D.U. This should be compared with the dominating effect of the solar height where the DUV spans over four orders of magnitude. An increase of the solar height from 10 to 50 degrees will increase the DUV a hundred times.

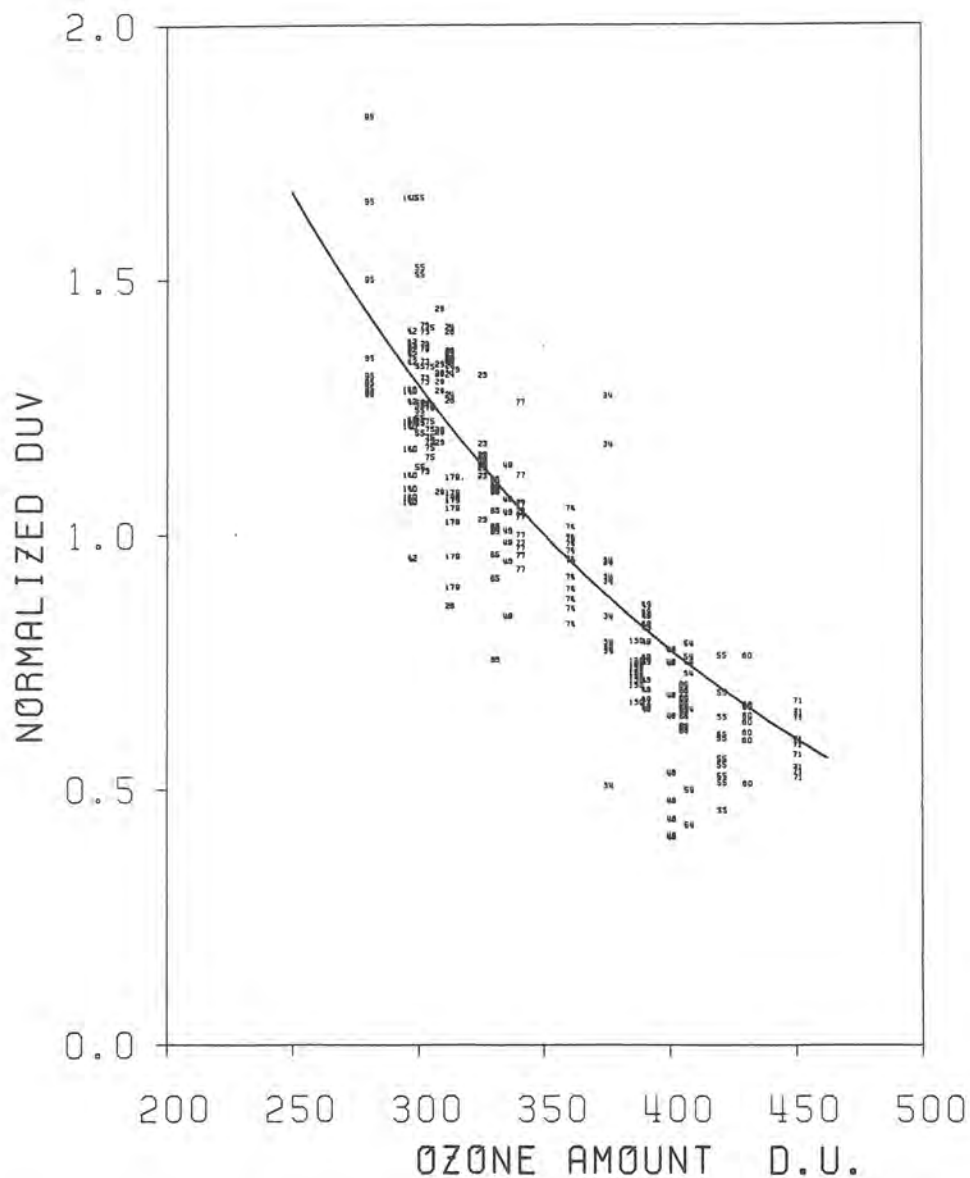


Figure 4.2 Hourly values of relative DUV as a function of the column amount of ozone for clear days. The plotted numbers are the measured Ångström turbidity coefficient of that day. The scatter in this figure is caused by variation in ozone, turbidity and there has also been some influence by thin clouds. The full line shows the relation used in the report.

4.3 Ground reflectance

The ground reflectance or the ground albedo is here defined as the reflected global irradiance relative the incident global irradiance and it is often given in percent. The spectral interval has to be specified.

SURFACE	REFLECTANCE IN UVB (%)
Fresh snow	70-95
Old snow	40-70
Bright dry sand	17
Water	5-10
Water above sand	10
White skin	1
Most vegetation	2-5
Clouds	20
Atmosphere	30

Table 4.1 Reflectance values in the UVB for various surfaces from Doda and Green (1981) and Beuttner (1969).

Most natural surfaces have a low reflectance in the UVB, about 5%. There are exceptions such as bright sand (10-20%) and snow (40-95%). A popular misconception is that water also has a high reflectance, but as can be seen in the table above it is as low as 5-10%. People engaged in activities in and around water, or sailing, are kept cool by the water and the wind. Therefore they will stay longer in the sun than elsewhere. However, there might also be a physical explanation, at large angles of incidence of the radiation total reflection occurs, i.e. a reflectance of 100%. For a very low sun the reflectance of the direct radiation is very high, but at these solar heights the direct UV is small. Waves and ripples on the surface of the water will increase the reflectance. Probably the magnitude of this effect is small.

The penetration of UV-radiation into water is high. Therefore being under the surface of the water when bathing will not give protection against sunburn under a high sun.

On the 11th of March, 1985, 10-13 local time reflectance measurements over fresh melting snow were performed. The snow fell during the night. A few Cirri were in the sky, but the sun was out of clouds. The instruments made by Wester were used in upward and downward positions. One and a half meter above a snow covered roof, about 90% of the viewed area (see Latimer, 1972) was covered with clean snow, the reflectance at 306 nm was 70-80% and at 360 nm the reflectance was about 68%. Having the downward looking instrument only 40 cm above the snowsurface it could be expected only to see snow. The reflectance at 306 nm was measured to 80-83%. A fresh and dry snowsurface will reflect almost all the downward DUV giving high irradiances even on surfaces not directly facing the sun.

The reflectance of snow depends on its state. Fresh and dry snow will give the highest values. Old, wet and dirty snow of course give low values, but in most cases it has still a higher reflectance than most other natural surfaces. Therefore the DUV irradiation will be significantly different if snow is present or not. A man standing, on a clear day, above a snow cover will receive substantially more radiation on all sides than he should if the snow cover was not there.

One should also note the difference of the local reflectance and the regional reflectance. The last concept is used in the model of Chapter 6 to describe the increase of DUV caused by snow covered ground. The regional reflectance is the average reflectance of a large area including trees, houses, fields etc.

Due to multiple reflections between the surface of the earth and the sky, with or without clouds, there will be an increase of the DUV-radiation on a horizontal surface if the regional reflectance of the ground increases. Assuming an average regional reflectance of 60% with snowcover present and an average sky reflectance of 25% the increase of the DUV will be about 16% compared to the same conditions without a snowcover. In open areas with large snowfields and a fresh snowcover the regional reflectance of the ground may be 80% and the increase of the DUV will be about 25%.

4.4 Clouds

The study of the influence of clouds was adapted to the model (chapter 6) that was going to be used for the mapping of DUV in Sweden. Therefore only the total cloud amount, given as the sum of the observations 07, 13 and 19 local time, was considered.

Using the model for clear skies on days with measured column amount of ozone and measured or estimated turbidity it was possible to determine the relative daily DUV. It was plotted versus the sum of the total cloud amount. The result is illustrated in Figure 4.4. Plotting almost all days of 1984, where the clear sky DUV was based on the model, gave a similar result only with a larger scatter. The scatter is mainly due to the imprecise description of the cloudcover during the day by only using three observations and that the type of cloud varies a lot. There is a big difference between a sky covered by cirri and a sky full of cumuli-ni-bi. The reason of using this rough cloud parameter is that there exist a useful database with the number of clear days and the number of overcast days, that are defined by using the sum of total cloudiness. Using the definition Figure 4.4 is divided in three parts and for each group of data the median value was determined. These three values were supposed to be representative cloud transmission values for the three types of days, namely a clear day (0.98), a broken day (0.84) and an overcast day (0.50). There has also been estimated a continuous function for the data set describing the relative DUV as

$$\text{DUV}(c)/\text{DUV}(0) = 1 - 0.7 \cdot C^{2.5} \quad (4-1)$$

where C is the total cloudiness. It gives a more condensed picture of the DUV dependence of the cloudiness. Even when the sky is covered more than half of clouds more than 80% of the DUV reaches the ground. More astonishing is perhaps that when the sky is almost completely covered by clouds still 50% of the DUV will reach the ground. This relation also seems to be applicable on hourly values. Because of the large scatter it should only be used for average conditions.

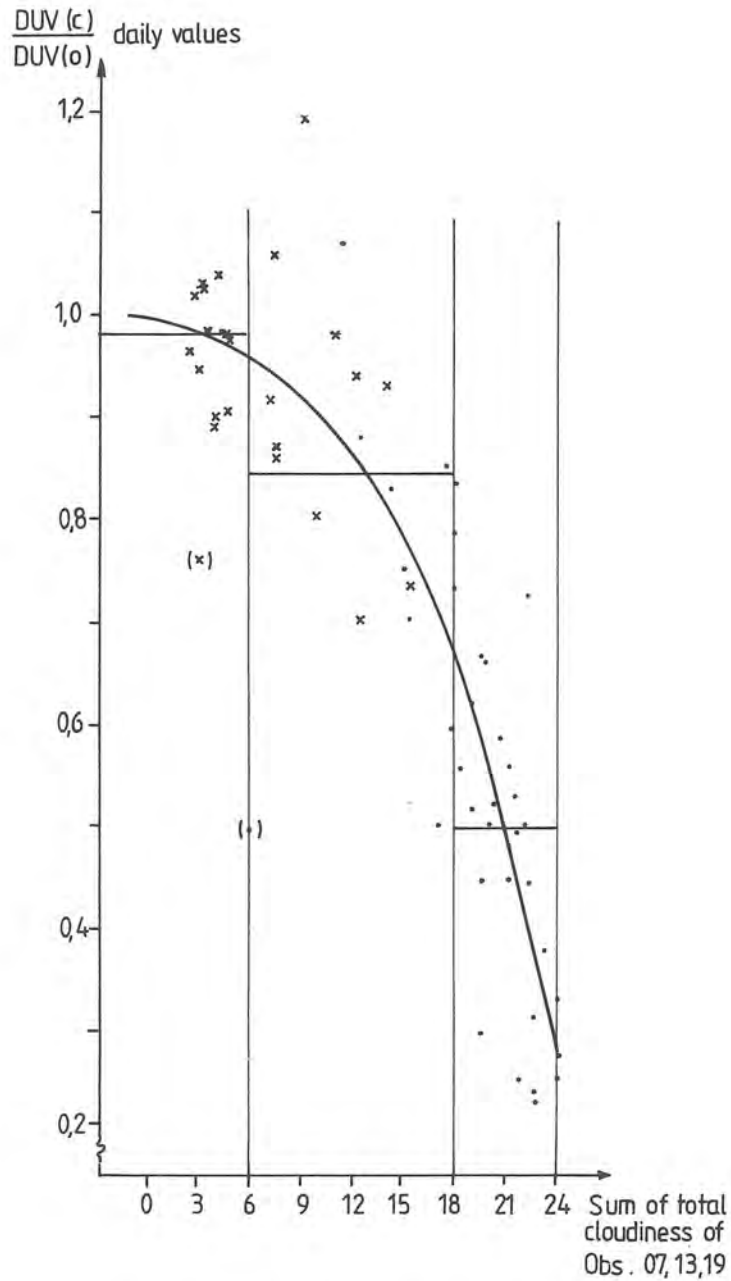


Figure 4.3 Relative DUV as a function of total cloudiness. The type of ozone observation is indicated by x for direct sun and as • for zenith sky observations. The days within parenthesis were found to be more cloudy than the observations at 07, 13 and 19 local time indicated. The solid line is the proposed continuous function to describe the relation. The three bars give the median value of each day type.

4.5 Turbidity

The lack of appropriate data made search of a relation describing the influence of aerosols to an ambiguous work. The atmospheric content of aerosols is here expressed by the turbidity coefficient of Ångström. The data had to fulfil certain criteria namely: no clouds, known amounts of ozone and turbidity. Then the selected measured values of DUV were corrected to the solar heights of 10, 20, 30 and 40 degrees. For each solar height the DUV values were plotted versus the turbidity with the ozone as parameter. Figure 4.5 illustrates the result for 30 degrees. Because of the small number of data the lines of equal amount of ozone are drawn by eye with the rough assumption of parallelity. However, there is no doubt of a decrease of DUV with an increase of the turbidity.

The range of variation of turbidity is wide. In Sweden the air sometimes is so free of aerosols that the turbidity almost reach the value of zero. High values of turbidity for swedish conditions is around 0.250. The value of the function used to describe the effect of turbidity on the DUV has the approximate range 0.7 to 1.07. For big cities local pollution contributes to a high content of aerosols. The attenuation of UV radiation might be considerable, due to scattering and absorption.

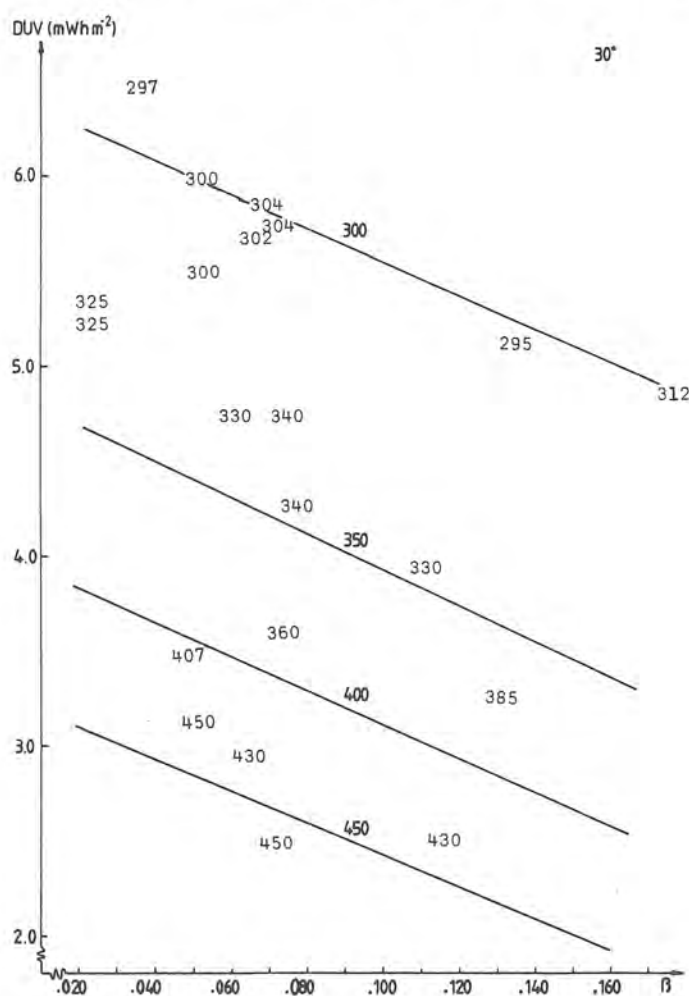


Figure 4.4 DUV as a function of the Ångström turbidity coefficient for solar height 30° and with the column amount of ozone as parameter.

4.6 Altitude

Ultraviolet radiation increases with increasing altitude. The increase is greater for shorter wavelengths due to the more effective scattering of these wavelengths. The altitude dependence of the DUV was not possible to evaluate from the measurements recorded in Norrköping. For moderate altitudes the dependence can be approximated by a linear equation as

$$\text{DUV}(H) = \text{DUV}(0) * (1 + p*H)$$

where H is the altitude above mean sea level in km. Using the data presented by Doda and Green (1981) p was estimated to 0.05, i.e. 5% increase per km.

5 RESULT OF THE MEASUREMENT

5.1 UVA Solar Radiation

Measured monthly values of the UVA irradiance on a horizontal surface in Norrköping are given in Table 5.1. The instrument used is described in section 2.2.1.

	1983	1984	1985
JAN		667	-
FEB		1380	-
MAR		3700	2901
APR		5823	5005
MAY		7580	8168
JUN		8911	7670
JUL		9495	8574
AUG	8136	6730	5967
SEP	3870	3574	3948
OCT	2279	1606	2097
NOV	910	680	758
DEC	406	-	412

Table 5.1 Monthly values of UVA in Norrköping 58.58N, 16.15E
Unit: Whm⁻²

The records of UVA and global radiation have been analyzed to determine if there is a relationship between the two. The fraction of UVA relative to global radiation has been computed for daily values. Also recorded is the state of the sky, here expressed as the average of total cloudiness for the observation terms 6, 12 and 18 UTC. It is a rough but in many cases sufficient parameter, because it is available at many sites.

Table 5.2 gives the minimum and the maximum percentages of the daily fraction of UVA for each month during the period January to November 1984 and average monthly fraction. To the maximum and the minimum values the corresponding daily average of the total cloudiness are given. Average total cloudiness values corresponding to the minimum and the maximum UVA/G values are also given.

It can be seen that the average monthly fraction is relatively constant with slightly higher values in the winter. The maximum daily fractions correlate with overcast days (7-8 octas) and the minimum daily fractions correlate with less cloudiness (note that even thin clouds are reported in the cloudcover and consequently contribute to the total cloudiness). The reason for this correlation is found in the scattering and absorption properties of solar radiation. Increased cloudiness favours shorter wavelengths dominating the diffuse component and disfavours longer wavelengths dominating the direct component.

The conclusion is that the UVA (315-400 nm) fraction of the yearly global radiation is 5-6%. Cloudy days will have a higher fraction than clear days. These facts make it possible to estimate UVA radiation at sites where the global radiation and the cloudcover are recorded. The UVA can probably be predicted with an accuracy better than 10% on a monthly basis. Long term averages will of course have a better accuracy. Comparison with data measured with Eppley UV radiometer 295-385 nm

from the Nordic countries, Kvifte et al (1983), show that the UVA-fraction is of this magnitude (5-6%).

1984	UVA/G (%)			AVE C AT	
	AVE	MIN	MAX	MIN	MAX
JAN	6.1	4.0	10.0	4.6	7.3
FEB	6.3	4.7	9.4	4.3	7.7
MAR	5.4	4.5	7.8	1.3	8.0
APR	5.2	4.6	7.4	4.7	8.0
MAY	5.3	4.9	7.6	2.7	7.7
JUN	5.6	5.1	7.5	1.0	8.0
JUL	5.6	5.2	7.8	5.3	7.0
AUG	5.4	5.1	6.9	4.7	8.0
SEP	5.8	4.9	7.6	1.3	7.0
OCT		4.5	8.9	3.4	8.0
NOV		3.9	8.2	1.0	8.0

Table 5.2 UVA in percent of global radiation in Norrköping 1984 JAN-NOV. Monthly averages and the minimum and the maximum of daily values. The corresponding average total cloudiness (octas) is given in the last columns.

5.2 UVB solar radiation

Measured monthly values of the UVB irradiance on a horizontal surface in Norrköping are given in Table 5.3. The instrument and the method of measurement are described in sections 2.1.1 and 2.1.3.

	1983	1984	1985
JAN		1.8	-
FEB		10.1	-
MAR	25.0*	33.5	26.8
APR	45.5*	76.1	63.8
MAY	104.0*	116.7	130.9
JUN	160.0*	155.7	150.5
JUL	219.7*	178.0	171.2
AUG	161.7*	128.4	115.8
SEP	55.9*	50.4	60.5
OCT	22.4*	14.6	26.1
NOV	5.8	4.2	-
DEC	1.3	-	-

Table 5.3 Monthly values of UVB in Norrköping, 58.58N, 16.15E. Unit: Whm^{-2} , * indicates interpolated value.

As described in section 5.1 the UVA is highly correlated with the global radiation. This correlation is not valid for the UVB which is highly affected by ozone, (section 4.2). This can be seen by studying the yearly course of the UVB as presented in Figure 5.1. Normally for solar radiation the maximum values are close to the solar summer solstice, i.e. the maximum solar altitudes. In this case the maximum of the UVB is shifted from the end of June to the mid of July. This is explained by the yearly course of the atmospheric content of ozone, showing that the combination of solar altitude and ozone is most favourable in July for the occurrence of high UVB-values.

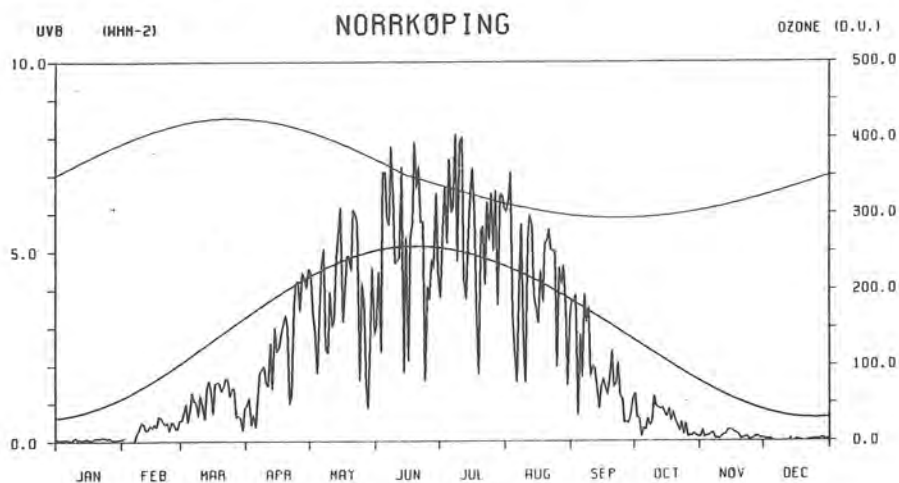


Figure 5.1 The yearly course of daily values of UVB in Norrköping during 1984. The average yearly variation of the column amount of ozone is plotted, upper curve, as well as the variation of the noon-solar height in Norrköping, lower curve.

5.3 DUV solar radiation

As the DUV is measured with different instruments two tables with monthly values are given. The discrepancy in the corresponding values of the two tables is discussed in section 3.2. In the following DUV values are from the Brewer records.

	1983	1984	1985
JAN		18	-
FEB		115	-
MAR		401	315
APR		1106	884
MAY		1837	2618
JUN		2763	2781
JUL		3338	3216
AUG		2383	2119
SEP		817	959
OCT		196	369
NOV	68	51	-
DEC	16	-	-

Table 5.4 Monthly values of DUV in Norrköping, 58.58N 16.15E, measured with the Brewer instrument. Unit: mWhm^{-2} .

	1983	1984	1985
JAN		18	-
FEB		113	-
MAR		389	308
APR		926	759
MAY		1458	1883
JUN		2043	1887
JUL		2578	2181
AUG	2457	1868	1477
SEP	849	701	716
OCT	305	173	294
NOV	69	47	49
DEC	13	-	16

Table 5.5 Monthly values of DUV in Norrköping, 58.58N 16.15 E, measured with the Wester instrument. Unit mWhm^{-2} .

The yearly variation of the daily values is given in Figure 5.2 as for the UVB in the previous section. The average yearly variation as computed by the model presented in section 6 is also plotted. It illustrates the great difference between long term averages and specific days. The average clear day values computed by the model (triangles) are close to the highest DUV values recorded. However, the computed extreme values (x) are far above the measured DUV values during the summer. This can be explained by higher amounts of ozone during the "bad" summer 1984 than the values used in the model (see Figure 5.7).

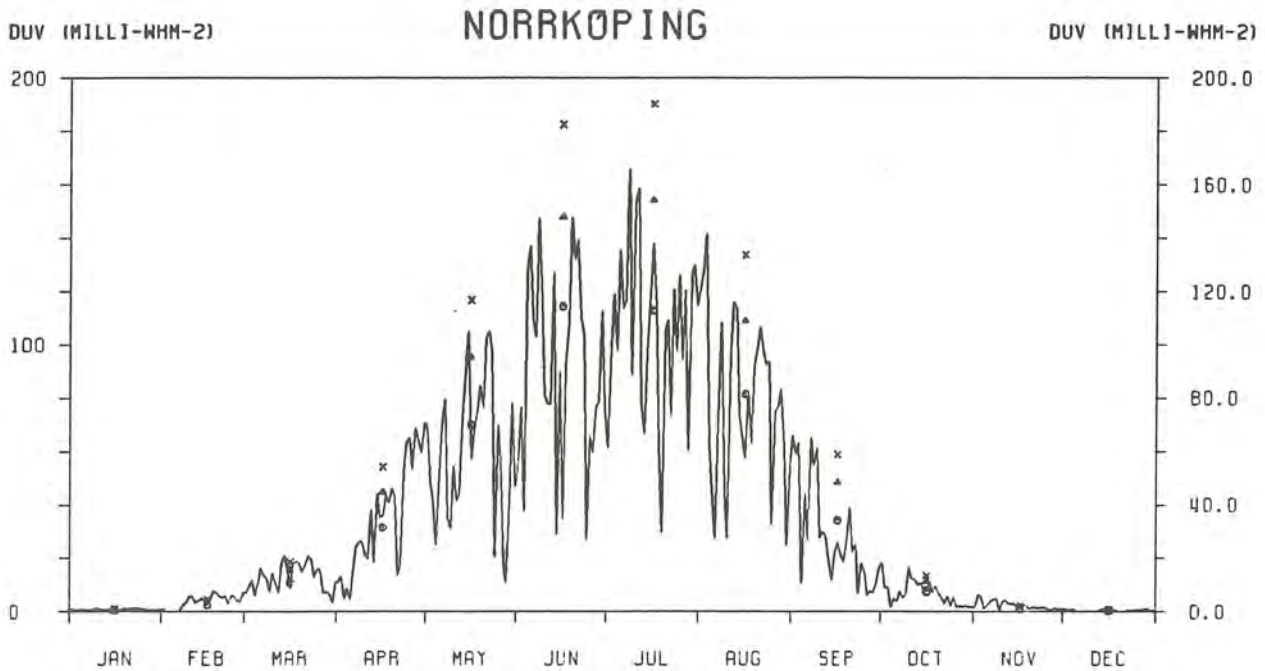


Figure 5.2 The yearly course of daily values of DUV in Norrköping during 1984. The monthly average daily values computed by the model described in chapter 6 are plotted as o. The corresponding average clear day values are plotted as Δ and computed extreme values as x.

The daily variation of some clear days is presented in Figures 5.3-5.4. The dominating dependence of the solar altitude is significant, both during a day and throughout the year.

In many applications the maximum values are of interest. Therefore the highest recorded daily and hourly values of DUV are put together in Table 5.6. Each month is divided in three parts to achieve a better description of the yearly variation. The given values are closely related to high solar altitudes and low values of the column amount of ozone. Note that the period of measurement is short and not complete. Therefore these values can only give a hint of the possible extreme values.

	MAX DAILY			MAX HOURLY		
	I	II	III	I	II	III
JAN	1.1	0.9	1.1	0.3	0.2	0.3
FEB	5.5	7.5	6.9	1.3	1.7	1.5
MAR	21.1	23.2	32.2	4.3	4.7	6.4
APR	46.8	63.5	70.3	8.8	12.1	12.4
MAY	115.4	136.9	145.8	19.1	22.4	23.2
JUN	165.3	147.6	149.5	26.4	25.0	23.8
JUL	170.7	158.8	129.7	28.5	27.9	21.5
AUG	141.4	116.1	97.4	22.4	20.9	18.4
SEP	65.2	60.1	36.3	11.5	11.5	7.6
OCT	26.9	15.8	11.0	6.1	3.5	2.6
NOV	6.3	4.4	1.6	1.5	1.1	0.5
DEC	0.9	0.7	0.8	0.3	0.2	0.2

Table 5.6 The highest recorded DUV values MAR 1983 - OCT 1985 with the Brewer in Norrköping. Unit: mWhm^{-2} . Each month is divided in three parts I (1-10), II (11-20) and III (21-end of month).

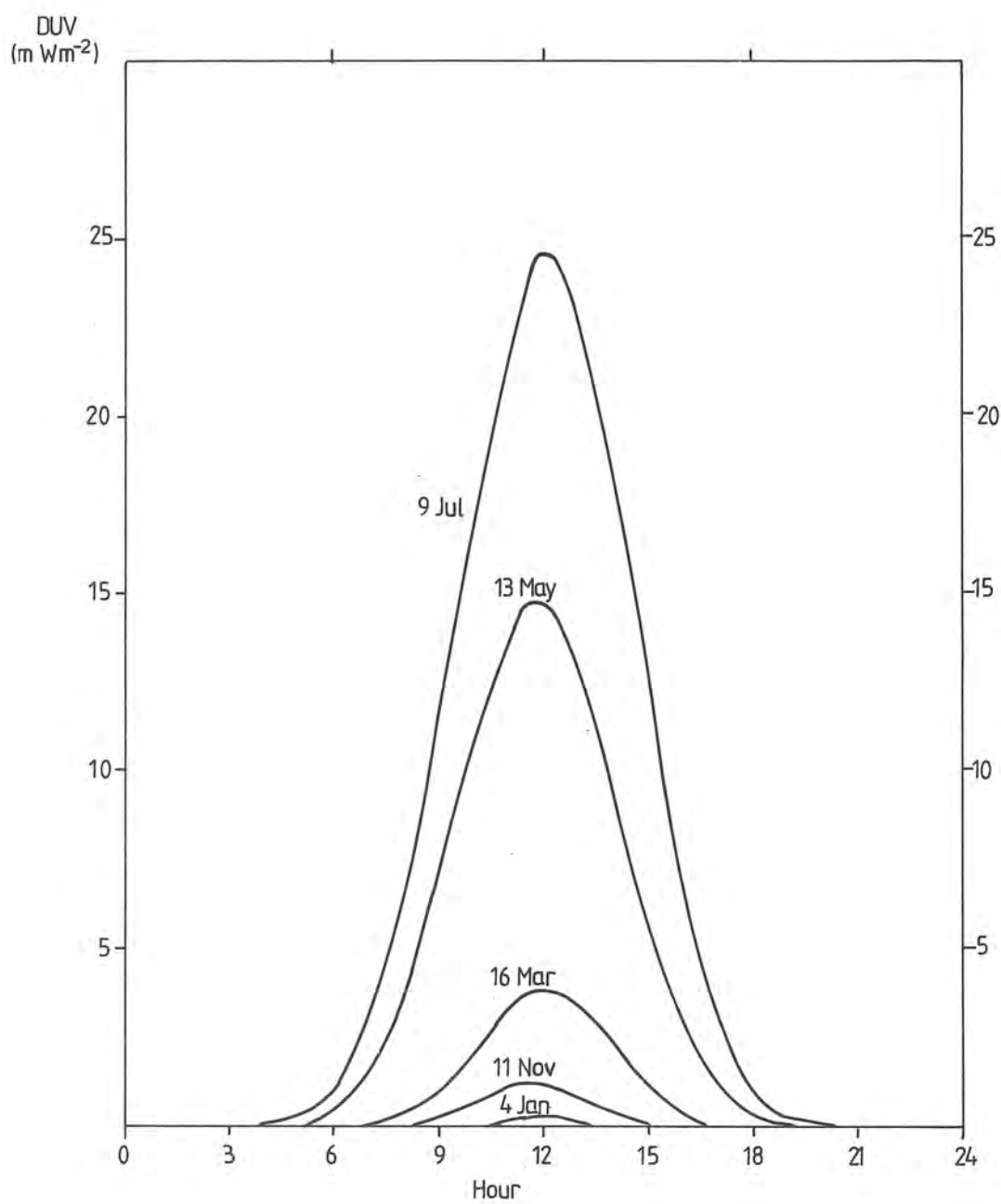


Figure 5.3 Measured DUV on a horizontal surface for some clear days in Norrköping.

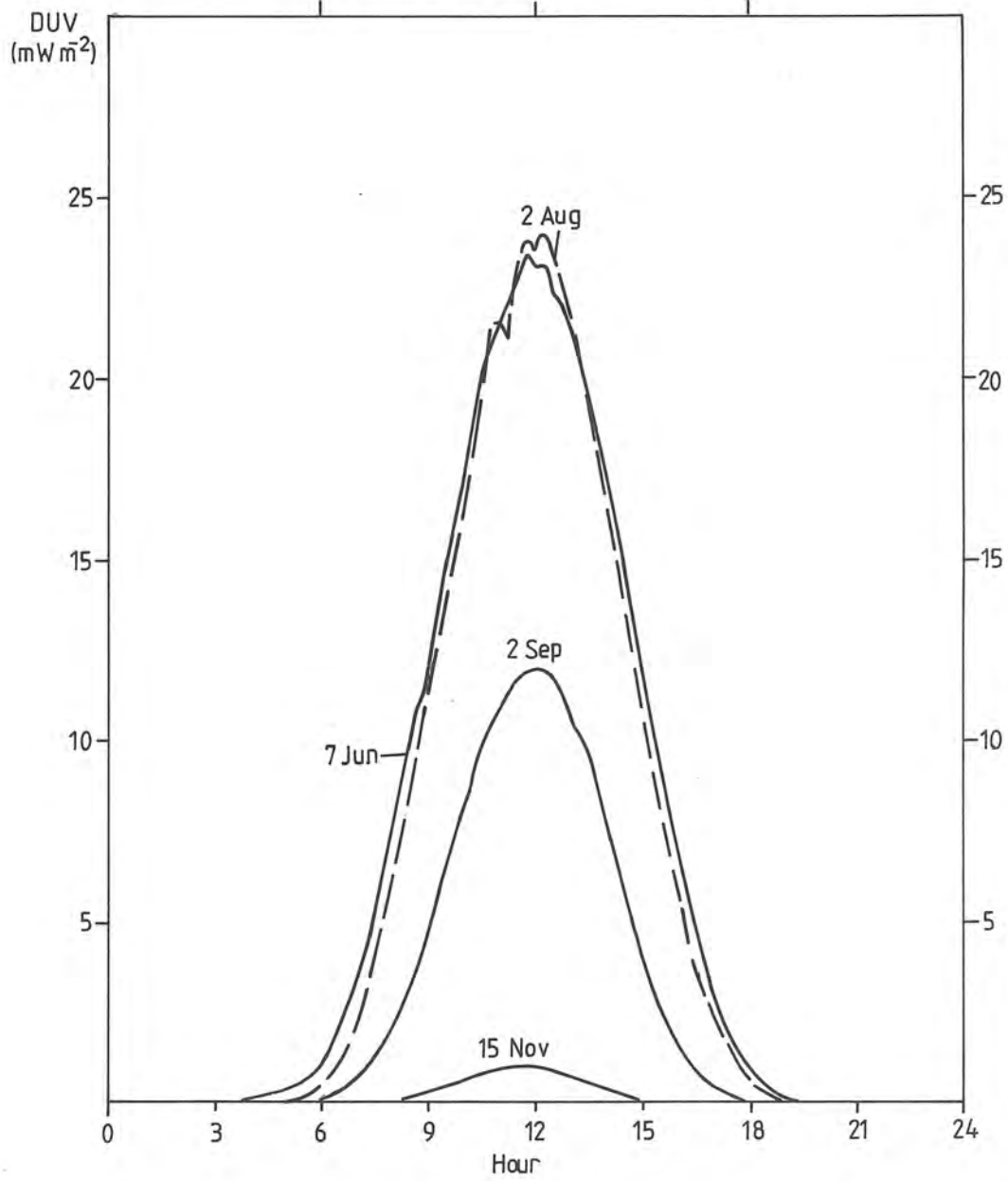


Figure 5.4 Measured DUV on a horizontal surface for some clear days in Norrköping.

The spectral composition of the DUV is exemplified in Figure 5.5. Note the logarithmic axis and the hatched area for wavelengths longer than 315 nm. In a linear plot this area will be relatively smaller and the irradiation with wavelengths longer than 315 nm are by definition not included in the DUV.

The depressions occurring in the spectra originate mainly from absorption lines in the extraterrestrial solar spectrum. In spite of the narrow band pass of the Brewer (0.6 nm) the measured spectrum is smoothed. A detailed solar spectrum would reveal a lot of individual lines in each dip.

Usually the DUV radiation will peak around 304-308 nm. Increasing solar altitude and decreasing amount of ozone will shift the peak towards shorter wavelengths. Consequently decreasing solar altitude and increasing amount of ozone will move it towards longer wavelengths.

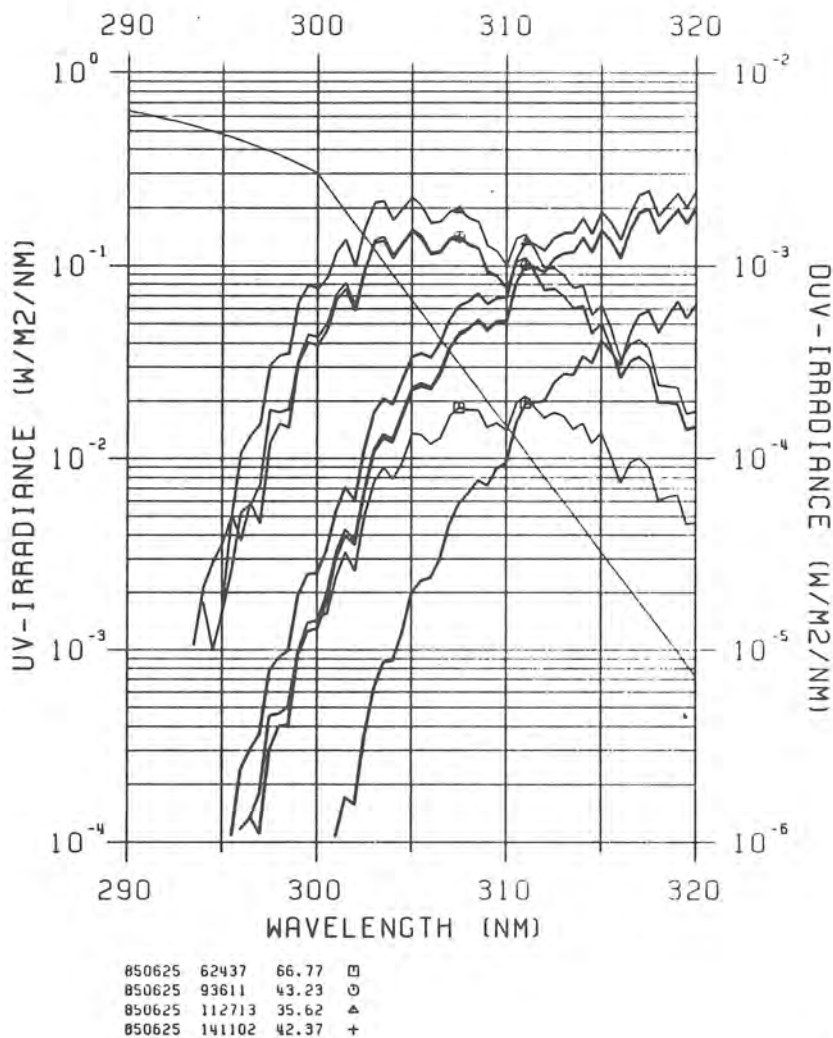


Figure 5.5 UV and DUV spectra for a horizontal surface in Norrköping. The relative response curve of DUV is also plotted. Date, time and solar zenith angle of each spectrum is given below.

5.4 Erythemal solar radiation

The erythemal response curve shows higher values for longer wavelengths than the ACGIH-NOISH-curve. To study if there is a simple relation between the erythemal solar radiation, ERY, and the DUV the factor (ERY/DUV) was recorded. The factor varied not only with the solar altitude but also with the column amount of ozone. The result of the study is presented in Figure 5.6.

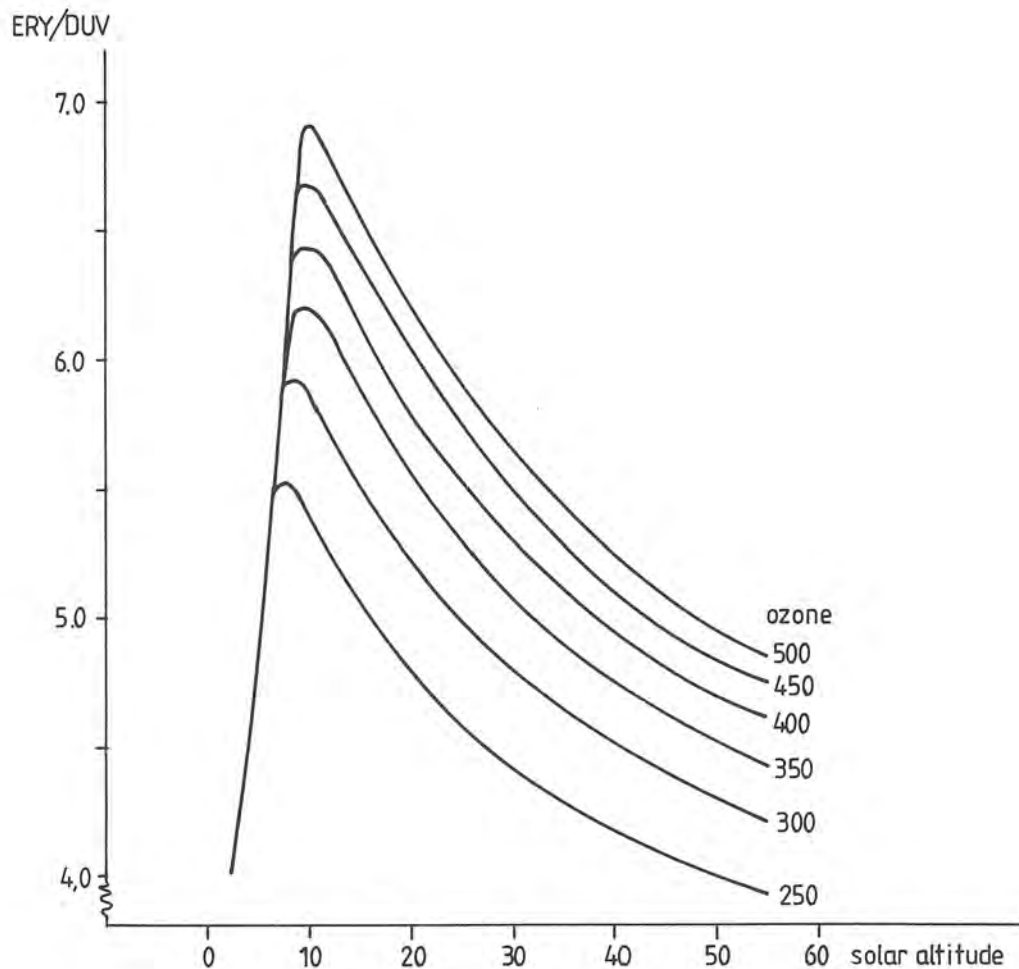


Figure 5.6 ERY/DUV as a function of solar altitude and the column amount of ozone.

In general the erythemal irradiation and the DUV-irradiation during a day is concentrated to the hours around noon. To find out the average erythemal irradiance at a place in Sweden one can use the maps in the Appendix, and compute an average ozone value from equation 6-5b or pick it out of Figure 5.7 valid for Norrköping. A typical noon-value of the solar altitude can be computed as $ALT = 90^\circ - \text{lat} + \text{solar declination}$. During summer the daily values of ERY are about 4.5-5.0 times the DUV.

The spectral response of the radiometer of Robertson-Berger tries to resemble the erythemal action spectrum. However, since the spectral response of the radiometer has larger response at longer wavelengths the measurements is not exactly describing the ERY variation. Especially not for low solar altitudes where the UVB is relatively small. Therefore the data measured with this instrument are given as relative unit i.e. number of registered counts. The yearly course of 1984 is presented in Figure 5.7 also plotted is the longterm average column amount of ozone and the measured column amounts of ozone of 1984. Unfortunately, the ozone measurements are not complete but there is a sufficient number in the autumn to show that the ozone amount of this period in 1984 was larger than the average based on data from London and Bojkov (1963).

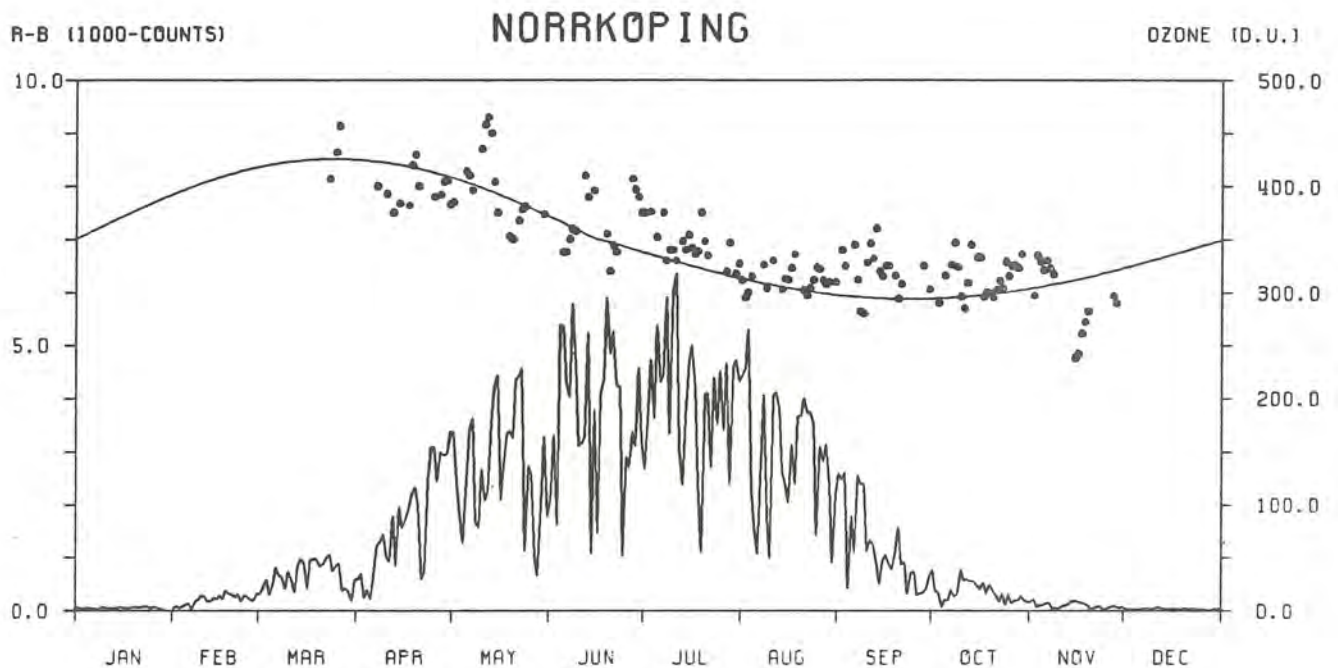


Figure 5.7 The yearly course of daily values of the Robertson-Berger Radiometer in Norrköping during 1984. Measured values of the column amount of ozone are plotted as well as a curve describing the average yearly variation.

5.5 UV spectra

The extraterrestrial solar UV-spectrum at high resolution shows a complicated structure of absorption lines. The measurements with the Brewer give a smoothed but still complicated picture of the spectrum at the surface of the earth. All measured terrestrial spectra in this report are global (diffuse + direct) spectra. Figure 5.8 illustrates the main and smoothed spectral properties for the wavelengths 280-400nm. The slowly increasing, with wavelength, extraterrestrial irradiance is attenuated in the atmosphere giving a terrestrial spectrum with almost no radiation below 300 nm. This sharp cut off is of course caused by absorption in ozone. The lower level of irradiance in the UVA range is mainly due to scattering. Also illustrated is the used response curve of DUV and the DUV spectrum. Data to Figure 5.8 are from measurements with an Optronic spectroradiometer, borrowed from SSI. More spectra recorded with this instrument covering the whole UV range of wavelengths are compiled by Wester (1983). The spectra measured with the Brewer are limited to wavelengths up to 320 nm.

As the spectral variation is large only a few typical examples will be given. Figure 5.9 illustrates that the variation with the solar altitude covers several orders of magnitude. Figure 5.10 illustrates that the effect of varying amount of ozone is small at wavelengths longer than 310 nm but it is significant at shorter wavelengths. It also illustrates that the effect of clouds seems to be almost independent of the wavelength.

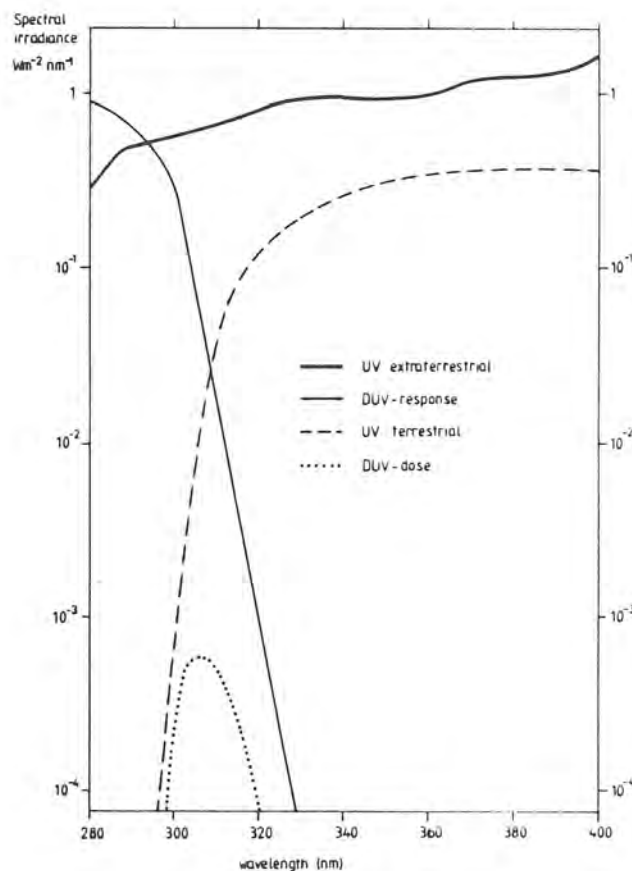
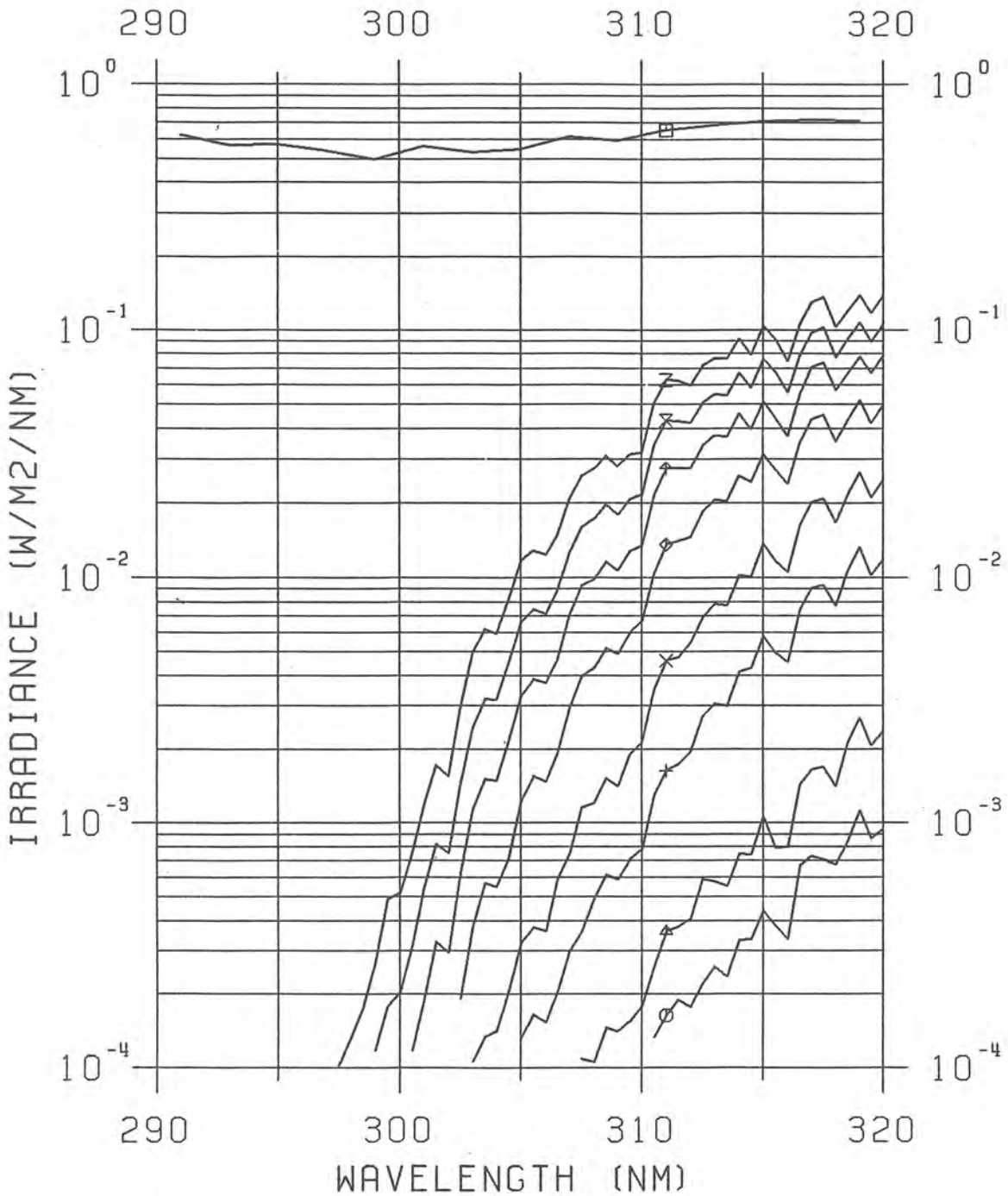


Figure 5.8 Main UV-spectral properties. Note the logarithmic irradiance-scale.



Extraterr. spectrum			□
850918	54148	89.41	○
850918	55813	87.27	△
850918	64212	81.58	+
850918	71528	77.38	×
850918	80530	71.41	◇
850918	85538	66.08	†
850918	94601	61.68	×
850918	115345	56.79	z

Figure 5.9 UV-spectra for different solar zenith angles on the 18th of September 1985, which was a clear day with a column amount of ozone of about 312 D.U. The top spectrum is the extraterrestrial. Date, time, zenith angle and symbol to identify each spectrum is added.

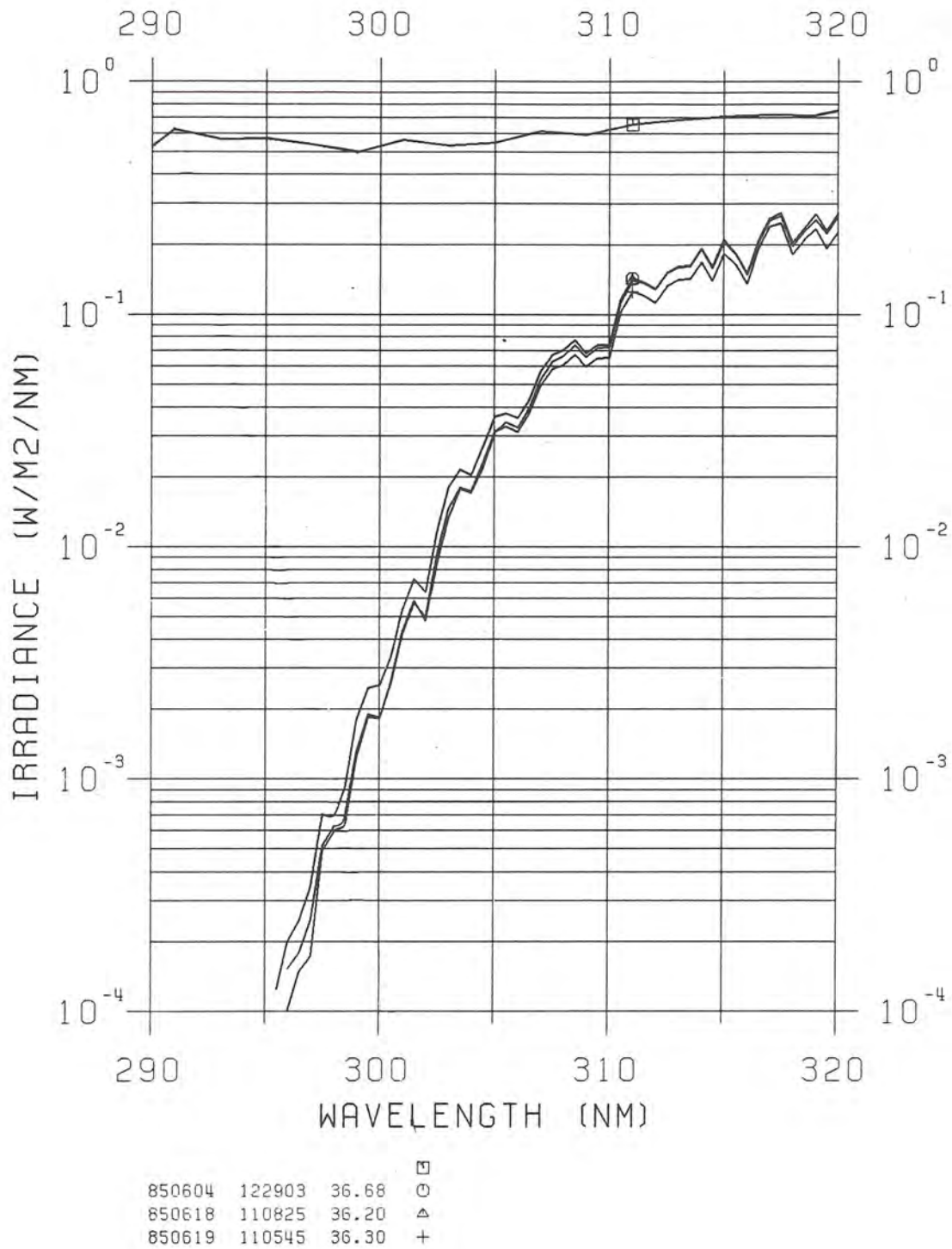


Figure 5.10 UV-spectra for almost the same solar zenith angle. The 4th of June 1985 was a clear day with a column amount of ozone of about 340 D.U. The 18th of June was also a clear day but with a column amount of ozone of 370 D.U. The 19th of June was a cloudy day with an ozone amount of 355 D.U. The top spectrum is the extraterrestrial. Date, time, zenith angle and symbol to identify each spectrum is added.

5.6 UV sky distribution

In connection with the testing of the deviation from true cosine - response of the Brewer it was interesting to know the distribution of the UV-radiation in the sky.

As the instrument body can be rotated in the azimuthal direction with the suntracker motor and the elevation can be changed with a stepping motor connected to the rotatable prism, the instrument can look at any part of the sky. By a simple program it was operated to turn in the azimuthal direction in step of 30 degrees. In each direction the movable prism was positioned at the zenith and at the elevations 75, 60, 30 and 15 degrees. Measurements were made in each direction at 310 and 320 nm. A scan of the sky is performed in about 10 minutes. The results is given as percentage of the average zenith irradiance.

Due to the polarization of the sky radiation caused by the Rayleigh scattering the Brewer is equipped with a polarizing prism, see Figure 2.1, which eliminates one direction of polarization. However, this will introduce an error when the instrument is used in the sky scanning mode. To solve this problem the quartz diffusor on one of the filter wheels was used as depolarizer and later a quarter wave plate (QWP) was inserted. However, the depolarizing effect of the quartz diffusor or the QWP is not proven.

Two examples are given. The first is a relatively overcast situation (7 octas of Stratocumulus). It reveals a characteristic pattern with decreasing irradiances towards the horizon and a minimum about 90 degrees from the sun in the vertical plane of the sun. Halfway from the sun towards the minimum there are two maxima. The maxima and the minimum are an effect of scattering and polarization but the darkening towards the horizon is caused by increased pathlength through ozone mainly in the troposphere.

The other example is also an overcast situation (8 octas of Cirrostratus), but the sun shines easily through these thin and high clouds. The basic pattern is similar to the first example except for the irradiance maximum around the sun.

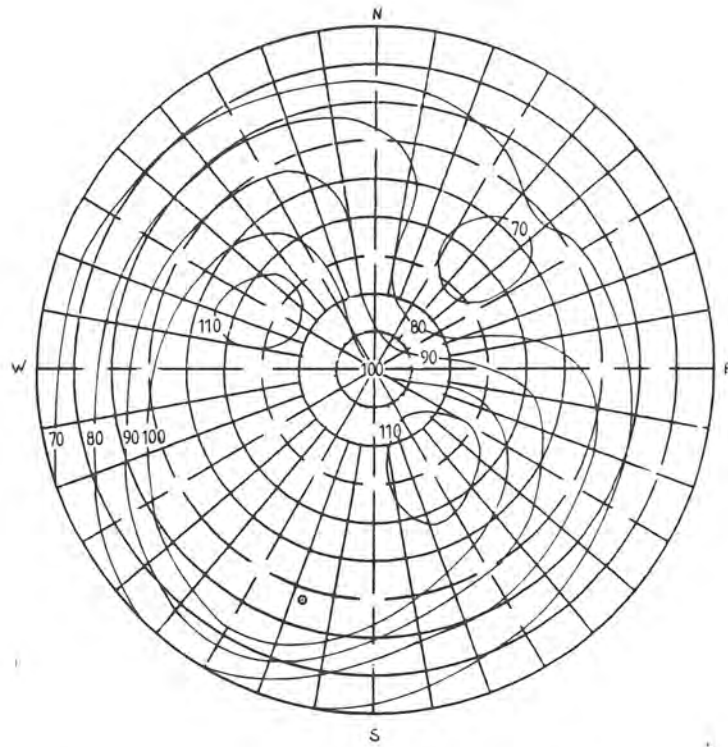


Figure 5.11 Relative UV-sky distribution at 310 nm. The zenith irradiance is 100. The clouds are 7 octas of Stratocumulus and the sun is positioned at 0.

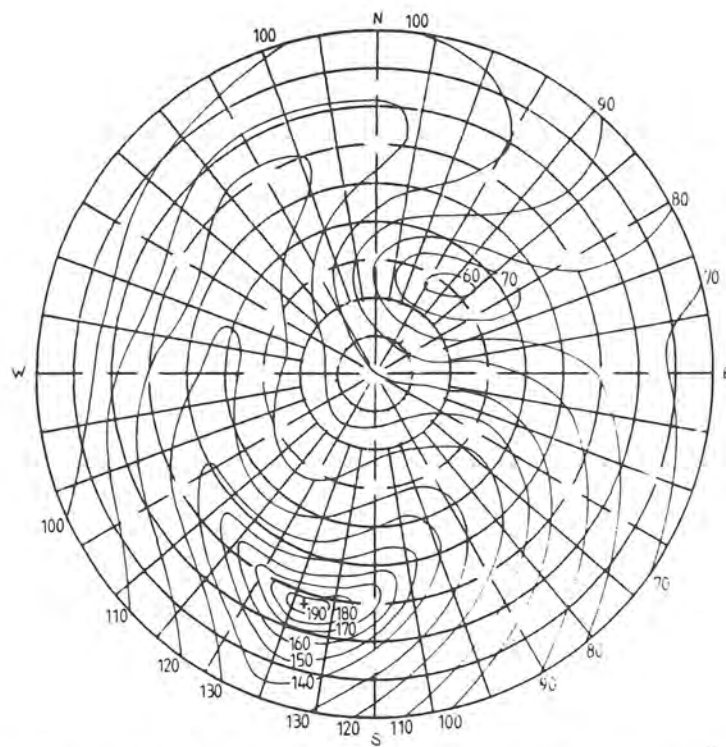


Figure 5.12 Relative UV-sky distribution at 310 nm. The zenith irradiance is 100. The clouds are 8 octas of Cirrostratus and the sun is positioned at +.

5.7 Ozone measurements

The Brewer has mainly been occupied with UV-measurements. Therefore the ozone records are spotreadings and the measurements have not been made daily. Despite this there is a lot of data. Only a selected part is presented in this report. The long term average in Norrköping is illustrated in Figure 5.7. The average range of variation is about 100 D.U., the maximum in spring is about 400 D.U and the minimum in autumn is about 300 D.U. Also plotted are the measured ozone values of 1984. The scatter around the long term average curve is significant.

The largest measured change of the column amount of ozone during a day occurred on the 17th of April 1984 when the amount increased with 15% from 390 D.U to 450 D.U. in about 4 hours. Synoptic weather charts revealed the passage of a polar jet stream, which probably caused a large transport of ozone from the stratosphere into the troposphere. Changes in the content of ozone of this order (50 D.U.) from one day to another are not rare. The highest observed values are close to 500 D.U and the lowest values are about 250 D.U. These facts point to the necessity of knowing the amount of ozone when making any computations of the attenuation of solar UV radiation for any specific time.

5.8 Sulphur dioxide measurements

Records of the column amount of sulphur dioxide, show that typical values are 0 to 0.006 cm in Norrköping. Enhanced values due to pollution are approximately 0.003 to 0.010 cm. An extreme enhancement was recorded on September 7, 1984, during the passage of a volcanic cloud. The maximum recorded value during the event was 0.042 cm. Air mass trajectories calculated backwards showed that the air over Norrköping originated from Iceland, where a volcanic eruption occurred a few days earlier, Figure 5.13.

A column amount of 0.001 cm over one square km corresponds to a volume of 10 m^3 of gas at STP (Standard Temperature and Pressure) or 28.6 kg of sulphur dioxide. For Sweden with an area of 450 000 square - km this amount corresponds to 13 000 tonnes of sulphur dioxide.

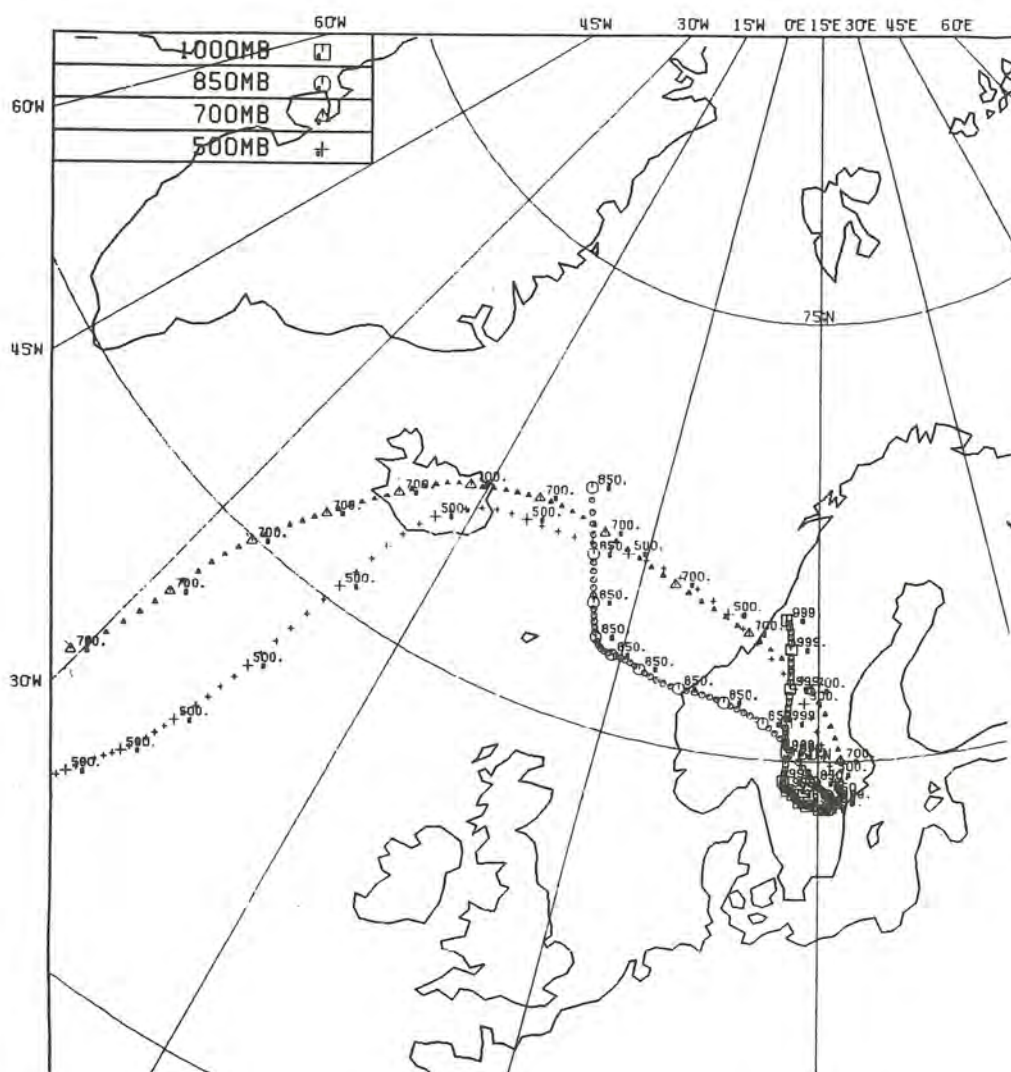


Figure 5.13 Isobaric backward trajectories from SMHI-LAM analyses starting in Norrköping at 12 UTC on the 7th of September 1984. Small symbols every hour, larger every 6th hour. Four levels are presented 500, 700, 850 and 1000 hPa. The trajectories were calculated by P Källberg, SMHI.

6 SPATIAL DISTRIBUTION OF THE DAMAGING ULTRAVIOLET SOLAR RADIATION

6.1 Description of the model

Assume that the damaging ultraviolet solar radiation (DUV) on a horizontal surface is a function of the earth's relative distance from the sun d , the solar height h , the column amount of ozone O_3 , the turbidity β , the ground reflectance α , the height above mean sea-level H and the cloud amount C . Of course there are other factors influencing the DUV but these are the main ones.

$$\text{DUV} = f(d, h, O_3, \beta, \alpha, H, C) \quad (6-1)$$

The next assumption is that this function can be separated in variables with the others given as constants, i.e.

$$\text{DUV} = f_1(d) * f_2(h) * f_3(O_3) * f_4(\beta) * f_5(\alpha) * f_6(H) * f_7(C) \quad (6-2)$$

The relative change in irradiance due to the earth's relative distance from the sun can be satisfactorily approximated by

$$f_1(d) = 1 + 0.033 * \cos(2 * \pi * \text{dnr} / 365.25) \quad (6-3)$$

where dnr is the day number (1-366). It can be seen that the non-circular orbit of the earth causes a variation of the solar radiation of 3.3% around the average with the maximum in the Northern hemisphere winter. The sun's output in the ultraviolet region of interest at the earth's surface is known to be stable within about 1%.

The solar height dependent function f_2 was evaluated from 'clear sky' data presented in Figure 4.1 The values are reduced to $O_3 = 350$ D.U., $\beta = 0.05$, $\alpha = 0.2$, $H = 0$ m and $C = 0$ and they have been fit to the following analytical expressions

$$f_{21}(h) = b * \sin^c(h) \quad \text{for } h > 15^\circ \quad (6-4a)$$

$$f_{22}(h) = a * 10^{d * \sin(h)} \quad \text{for } h \leq 15^\circ \quad (6-4b)$$

where $b = 48.782 \text{ mWhm}^{-2}$, $c = 3.3894$, $a = 0.0224 \text{ mWhm}^{-2}$ and $d = 5.211$. In the model the solar height is computed from the given latitude and longitude for the midpoint of each hour-interval.

The ozone dependent function is also deduced from measured values. This function will give a factor to correct the DUV if the column amount of ozone differs from 350 D.U.

$$f_3(O_3) = \exp(-0.005134 * (O_3 - 350)) \quad (6-5a)$$

The average column amount of ozone for each day of the year at a specific site in Sweden is approximated by the following set of equations, based on the measurements in Norrköping and on the data published by London and Bojkov (1963).

$$O_3 = A + B * \sin(\pi * (\text{dnr} + \text{phase}) / P) \quad (6-5b)$$

where $A = 350$ D.U., $B = 17.3 + \text{lat}$, $P = 167$, $\text{phase} = 0$ if $\text{dnr} = 168$ and $B = 0.333 + 0.95 \cdot \text{lat}$, $P = 198$, $\text{phase} = 30$ if $\text{dnr} = 168$, where lat is the latitude in degrees.

The aerosol influence is written as

$$f_4(\text{beta}) = 1 + k \cdot (1 - \text{beta}/b_0) \quad (6-6a)$$

where $k = 0.08$. By plotting clear day DUV-values for the same solar height as a function of the Ångström turbidity coefficient, beta , and also plot the corresponding value of the column amount of ozone it was possible to find a rough value of k for $b_0 = 0.05$, Figure 4.5. The function f_4 is about 0.70 for turbid conditions and about 1.07 for typical clear conditions in Sweden.

The spatial distribution of the average turbidity is parameterized in following way. The air is assumed to have decreasing content of aerosol with increasing latitude but the yearly variation is assumed to be similar.

$$\text{beta} = A + B \cdot \sin(2 \cdot \pi \cdot (\text{dnr} - \text{phase})/P) \quad (6-6b)$$

where $B = 0.018$, $\text{phase} = 91$ days, $P = 365$ days, $A = (31.0 + 1.0 \cdot (59 - \text{lat}))/1000$ and lat is the latitude in degrees.

The function f_4 is only approximating the average conditions because the normal variation of beta is large. A typical range of variation in Norrköping is 0.003 to 0.225 but the yearly variation of the average used in this model only have the range 0.013 to 0.050.

The influence of the surface and sky reflectance (albedo) is an important factor especially with snow-covered ground. As the other relationships are deduced for an ultraviolet reflectance of approximately 0.05, a correction has to be applied for days with snow-cover.

The influence of multiple reflection can be approximated by a factor F as

$$F = 1 / (1 - r_g \cdot r_s) \quad (6-7a)$$

where r_g is the ground reflectance and r_s is the sky reflectance. Assuming that snow-covered ground (including trees, buildings, etc) in common has a reflectance of 0.6 and that the sky has an average reflectance of 0.25, independent of the amount of clouds, the correction factor can be given as

$$f_5(n_s) = 1 + 0.16 \cdot n_s \quad (6-7b)$$

where n_s is the fraction of time with snow-cover during the month.

The simplifications may seem to be rather rough but the knowledge of the reflectance values of different surfaces is poor and the state of the ground in different parts of Sweden is not known in detail. The reflectance properties of the solar radiation in the atmosphere is especially interesting concerning the ultraviolet radiation. Due to the increase in scattering efficiency with decreasing wavelength the atmosphere itself has a reflectance of about 0.3. However, the scattering and absorption in clouds are more efficient in the visible region than in the ultraviolet region. This causes a lower reflectance of clouds in the ultraviolet, approximately 0.2 compared to 0.6 in the visible.

The correction for altitudes above sea level is given in the following form

$$f_6(H) = 1 + 0.05 \cdot H \quad (6-8)$$

where H is in km. This is a rough estimate calculated from data given by Doda and Green (1981) and it is only valid for heights below 2 km, which is sufficient in Sweden.

The parameterization of the influence of cloudiness is based on the measurements in Norrköping. Clear sky values calculated by the model have been used for the normalization of the measured daily values. These values are plotted versus the sum of total cloudiness for the observation terms 06, 12, 18 UTC (Universal Time Coord.). The reason of using this coarse cloud parameter is that the model will be used for mapping the distribution of DUV in Sweden and most stations only observe three times a day with the cloud observation only given as total cloudiness.

These cloud observations are used to classify the days in the following three groups. A day is considered as clear if the sum of octas (total cloudiness) for the three observations 06, 12 and 18 UTC is less or equal to 6 and as overcast if the total cloudiness is larger or equal to 18. The remaining days are considered as "broken". Average number of days within each of these classes are available for each month and for many stations in Sweden.

According to the definition above a clear day is not always a day free of clouds. The factor to reduce a value for a really cloud-free day to one for a clear day corresponding to the definition above is approximately 0.98. The factors for the broken day and for the overcast day were found to be 0.84 and 0.50 respectively. These are the median values found out of 60 days with known column amount of ozone, Figure 4.4. The use of the complete data set for 1984 did not introduce any significant change, although the scatter did increase. A similar result was found by Paltridge and Barton (1978) for the erythemal dose in Australia.

$$f_7(C) = (0.98 \cdot n_c + 0.84 \cdot n_x + 0.50 \cdot n_o) / (n_c + n_x + n_o) \quad (6-9)$$

where n_c is the average number of clear days, n_x is the average number of broken days and n_o is the average number of overcast days.

Using the set of equations given above and information of the average number of clear, broken and overcast days and the average number of days with snow-covered ground it was possible to compute the DUV-radiation for a large number of synoptic stations in Sweden for each month. These calculated values have been used for the drawing of the maps given in the Appendix.

As can be seen from Figure 5.2, describing the annual course of the DUV in Norrköping in 1984, the change during a specific month is considerable. The difference between two consecutive clear days can also be large if the amount of ozone changes. To give an impression of this phenomenon extreme values have been computed for a realistically low amount of ozone and also a low value of the turbidity coefficient. The average column amount of ozone was reduced by 25 D.U. and the Ångström turbidity coefficient was set to 0.010. The result points out that the natural range of variation is considerable. It also gives a hint of how large the increase of DUV would be if the average amount of ozone decreased by 5 - 10 %.

6.2 Comments to the maps

The maps describe the average DUV-distribution of each month. The input and the output parameters of the model are representing the period 1961 - 1983. Due to the large annual variation of the DUV irradiation the values of the isolines have been chosen differently for different months to give the best description of the geographical pattern.

In the mountainous area of the northwest of Sweden broken lines are used, because of the complex terrain.

To the left of each map and for each even degree of latitude two values are given. The upper value gives the average daily value of a clear day for the 15th of the month. The lower value is the maximum hourly value of this clear day.

Annual mean distribution

It should be observed that the unit of the yearly value is Whm^{-2} . The squares on the left give the corresponding average clear values as if there had been no clouds in the sky during the year. The latitudinal gradient is dominating, caused by the high dependence of DUV on the solar altitude.

Deviations of the isolines from being parallel with the latitude circles are almost exclusively a function of the cloud variability. Because of the large annual variation, with low values in winter and high values in the summer, the cloudiness conditions of summer will be the main factor of the non-parallelism. The effect of the difference in cloudiness between sea and land is favourable to the coast. This effect is also recognizable at the great lakes.

The dominating westerly winds of the mid-latitudes will cause an increase in cloudiness on the west side of mountains and a decrease on the leeward side (east). This will cause a tilt of the isolines relative to the latitude lines easily recognizable in the north and the south of Sweden. The decrease in DUV irradiation on the west side of the not very high mountains (peak 377 m) in the south of Sweden is very apparent. The lee effect of the mountains in the south of Norway is also clear.

Monthly distribution

It should be observed that the unit is $\text{mWhm}^{-2}/\text{day}$. Dominating features are the high latitudinal dependence and the large annual variation. The months of October to March are characterized by low irradiation and isolines practically parallel to the latitudes. However, the small difference in cloudiness between sea and land together with snow-covered ground give slightly higher values on land compared to the sea.

For the months of April to September the irradiation is higher and the differences in cloudiness between sea and land is evident. Most of the characteristics of the contours are explained in the section "Annual mean distribution" but some points should be emphasized. The coast and the great lakes have generally higher irradiation levels than the inland at the same latitude. There is a sharper gradient at the west coast than at the east coast.

Concluding remarks

The given values are average values for a long period. Therefore individual months can differ considerably from the given values. The large annual variation of DUV points at the fact that the DUV of the first day of a month usually differs a lot from the DUV of the last day. Average values for individual days may be found by plotting the annual course of the DUV. However, a value for a specific date found in this way is only to be used as an average value representative for a long period of time. Mainly due to variations in the ozone layer and in cloudiness conditions the DUV irradiance for a specific date can be completely different from one year to another.

6.3 Clear day data

As many human activities are connected with clear days some aspects of the DUV radiation of these days will be presented. The plots are based on data of the model described in section 6.1 and show the yearly variation of DUV for the latitudes in Sweden.

The main feature is the large difference between summer and winter with the rapid change around the equinoxis.

In Figure 6.1 the maximum hourly DUV value of an average clear day is given during the year and for latitudes in Sweden. The data of this figure can be used to compute the time to get a DUV-irradiation of 30 J m^{-2} (8.333 mWhm^{-2}) on a clear day, starting the exposure around noon. The result is presented in Figure 6.2. The chosen irradiation of 30 J m^{-2} is a rough approximation of the amount needed to cause a slight reddening of white skin.

To point on the difference between an average clear day and a day with low turbidity and a low amount of ozone three figures are presented. The first one, Figure 6.3, gives the daily DUV of average clear days and the second one, Figure 6.4, gives the daily DUV of a clear day with 25 D.U. lower amount of ozone and low turbidity. Figure 6.5 presents the difference in terms of latitude. A reduction of the ozone with 25 D.U. will increase the DUV-irradiation to a level that is equal to the average clear day DUV-irradiation of a more southern latitude. For example at the latitude of 65 degrees north in March this reduction of ozone corresponds to a latitude displacement of -1.5 degrees and in June and July it corresponds to a latitude displacement of -6 degrees. A discrepancy of 25 D.U. of the column amount of ozone from the average is not rare. The normal range of variation for daily values is about 50 D.U. around the average. However, a systematic decrease of the column amount of ozone would cause a notable increase of the damaging effects of the UVB and DUV-irradiation at the surface of earth.

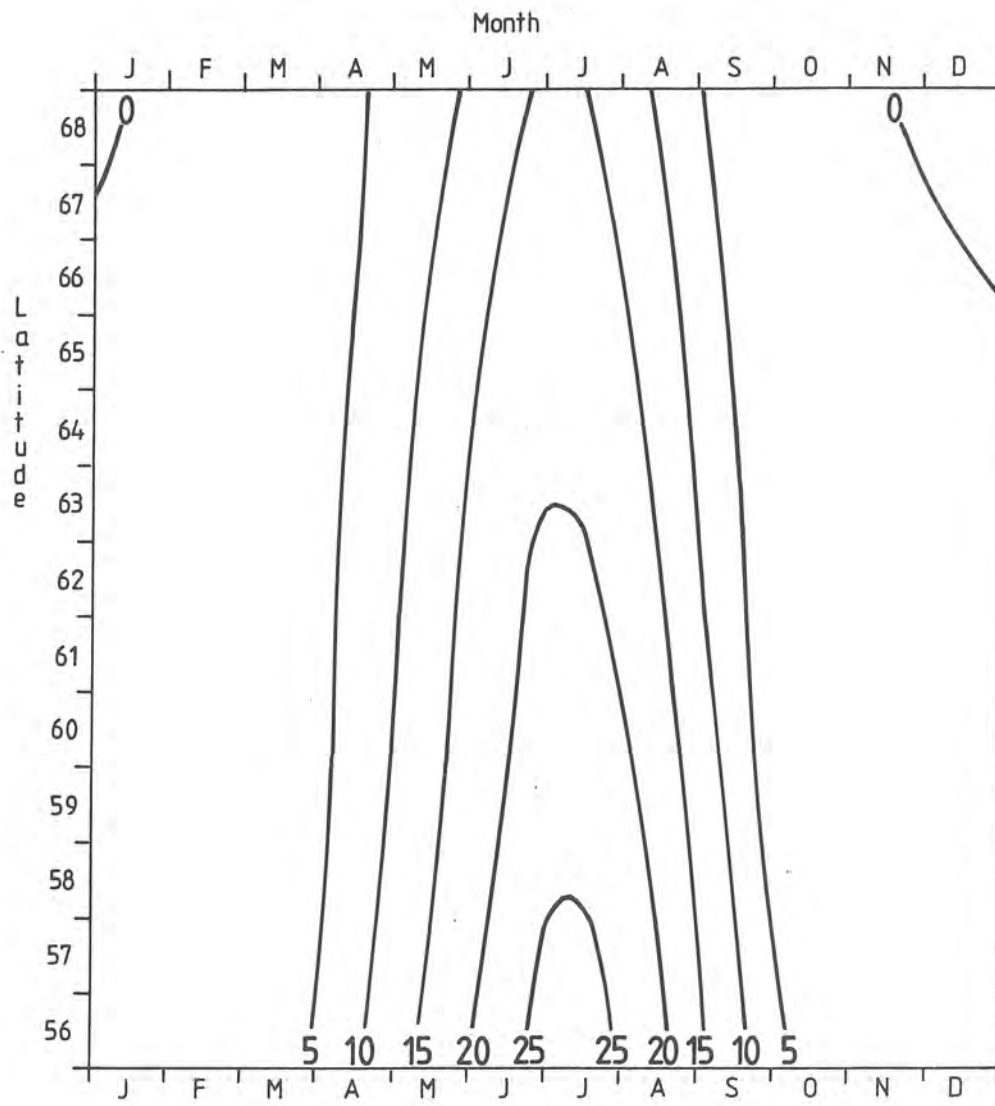


Figure 6.1 Maximum hourly DUV on a horizontal surface for an average clear day for each month and latitude in Sweden. Unit: mWhm^{-2} .

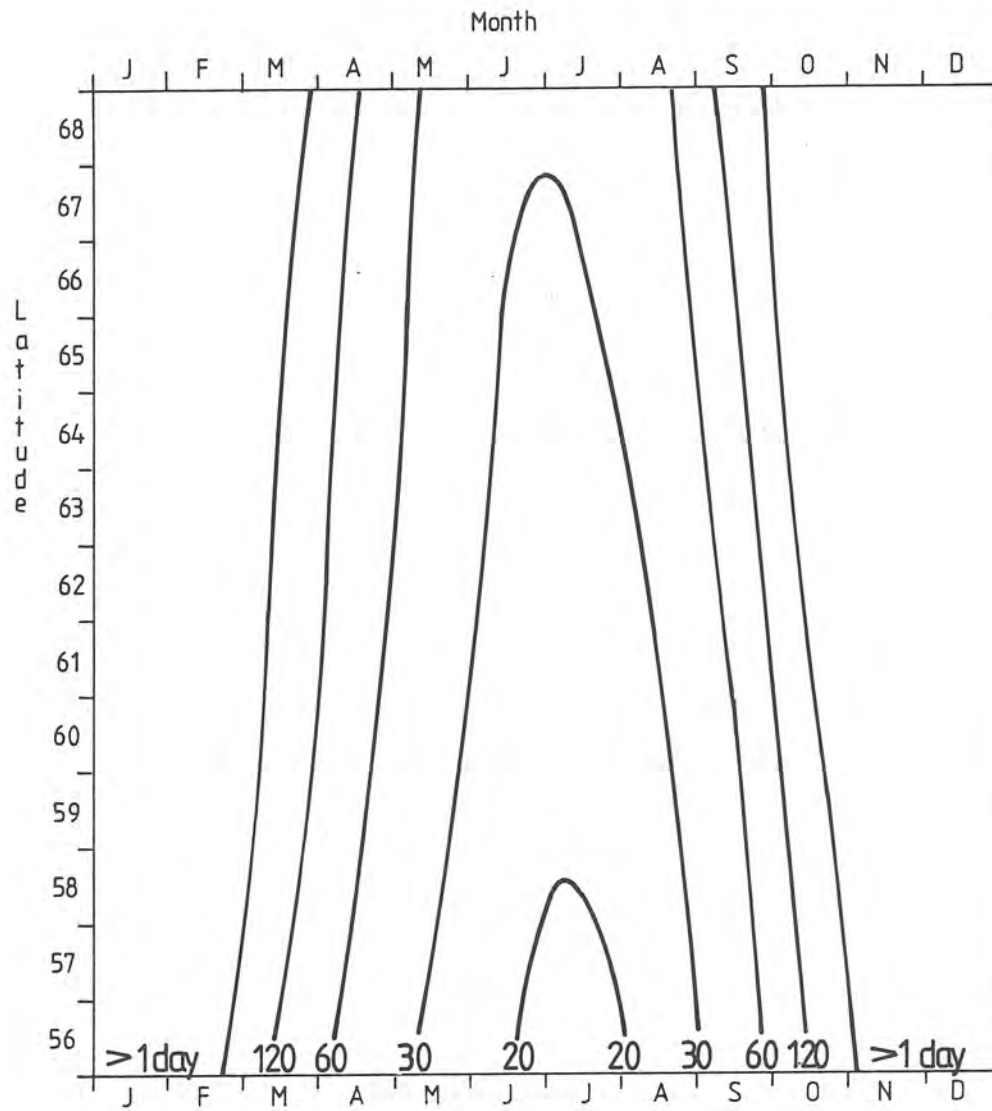


Figure 6.2 The time in minutes to get a DUV-irradiation of 30 Jm^{-2} (8.333 mWhm^{-2}) on a horizontal surface on a clear day starting the exposure at noon, for each latitude and month in Sweden.

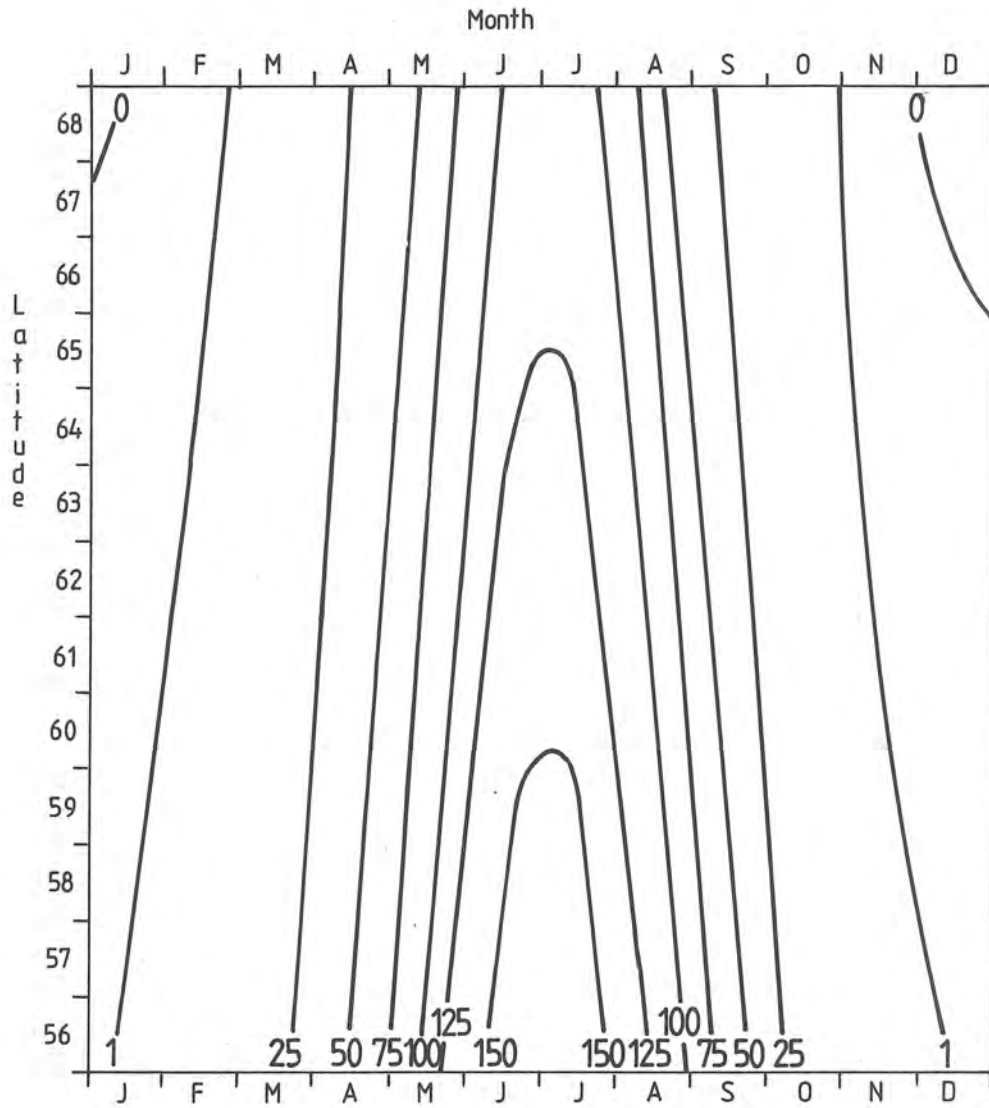


Figure 6.3 Daily DUV on a horizontal surface for an average clear day of each month and for each latitude in Sweden. Unit: mWhm⁻².

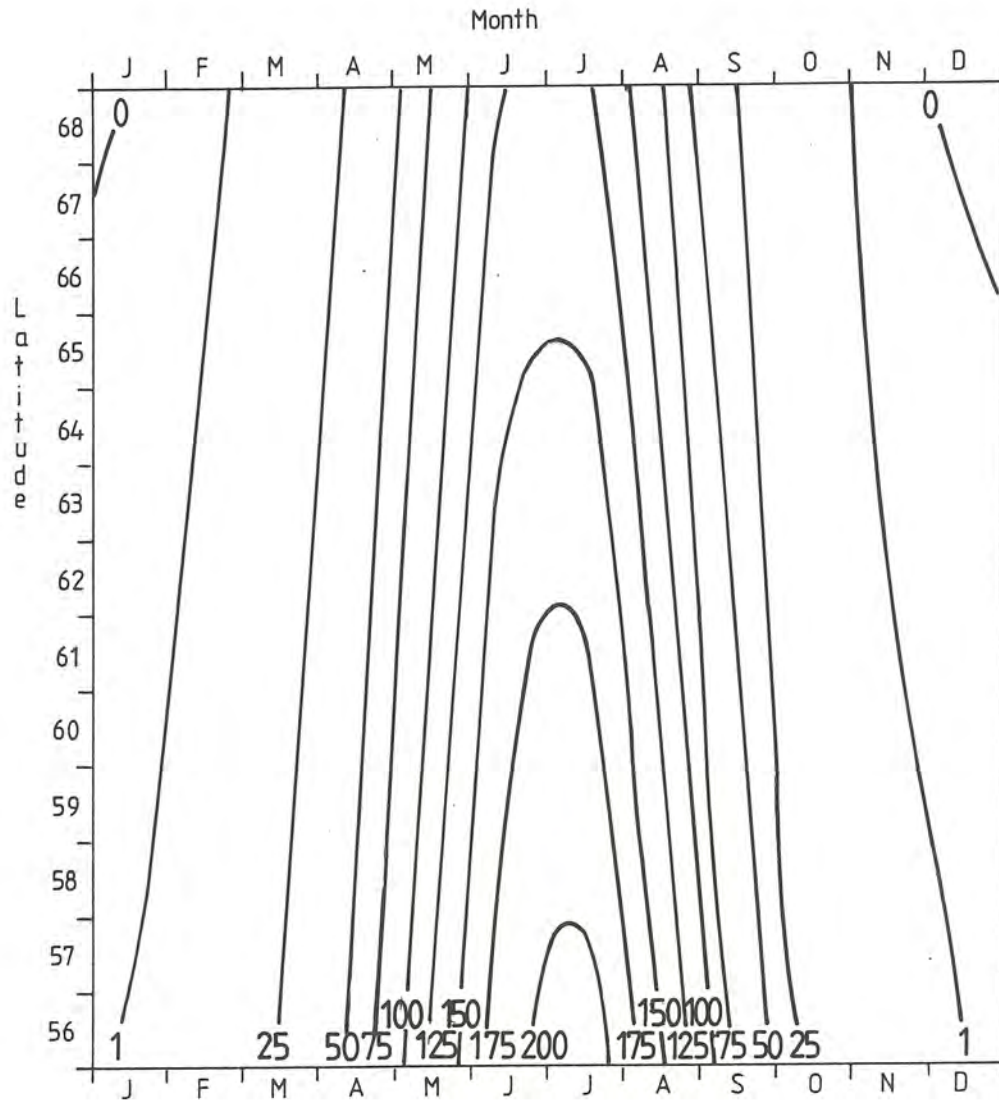


Figure 6.4 Daily DUV on a horizontal surface for an average clear day, with 25 D.U. lower column amount of ozone than the average, of each month and for each latitude in Sweden. Unit: mWhm^{-2} .

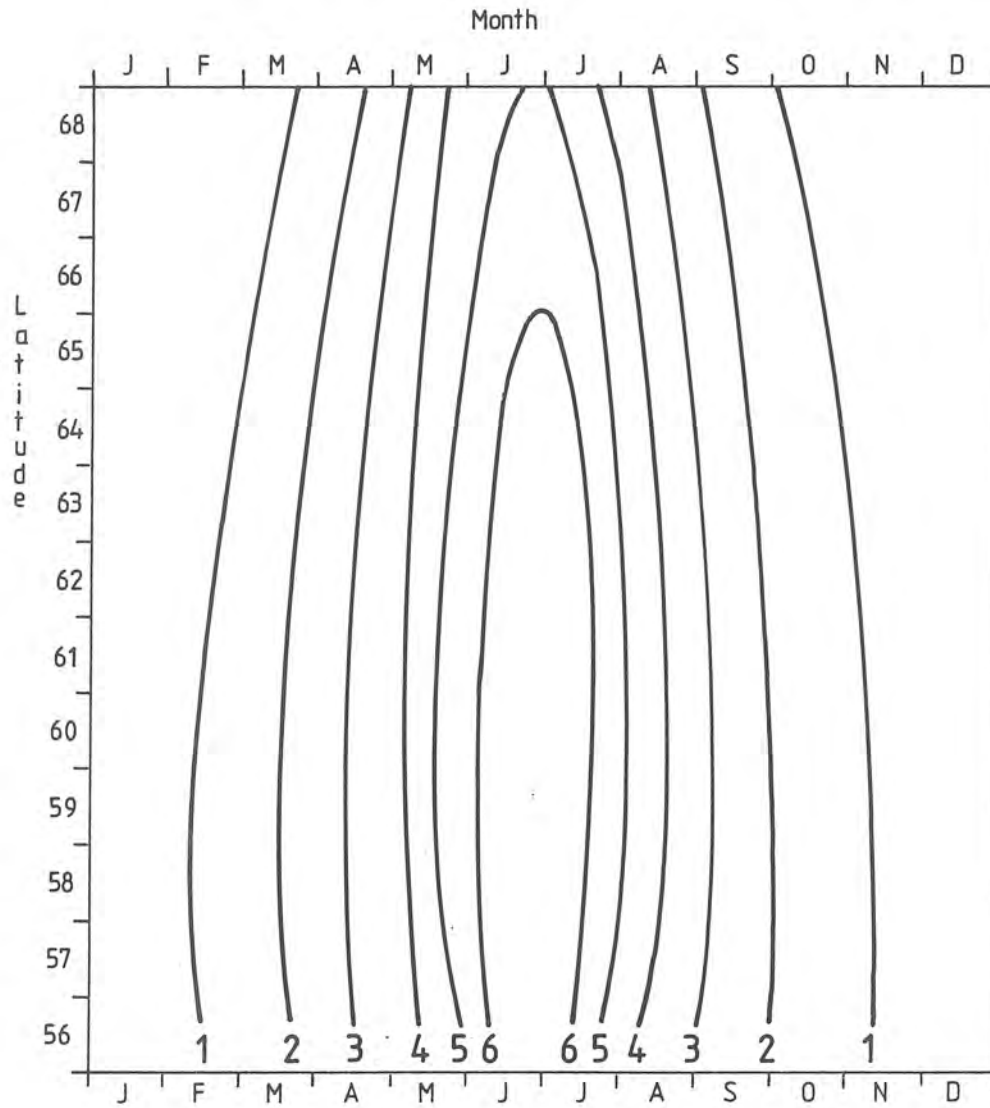


Figure 6.5 A reduction of the average column amount of ozone with 25 D.U. (6-10%) will increase the DUV irradiation corresponding to a decrease in degrees of latitude as illustrated in this figure for each month and latitude in Sweden.

ACKNOWLEDGEMENTS

The author wants to express his sincere thanks to the Swedish National Institute of Radiation Protection (SSI) for their sponsorship of this project. I hope that they will find a sign of my gratitude in the results of the present report. I am also greatly indebted to the designers of the instruments that have been used.

REFERENCES

ACGIH (1978), Threshold Limit Value for Chemical Substances and Physical Agents in the Workroom Environment with Intended Changes for 1978. American Conference of Governmental Industrial Hygienists, P.O. Box 1937, Cincinnati OHIO 45201, U S A, 1978.

Bacher R. E. (1982), Review of the Dobson Spectrophotometer and its accuracy, WMO Global Ozone Research and monitoring project, Report No. 13, Geneva, 1982.

Bener P. (1960), Investigation on the spectral intensity of ultraviolet sky and sun + sky radiation under different conditions of cloudless weather at 1590 m.a.s.l., Davos-Platz, Switzerland, Dec 1960.

Berger D. S. (1976), Photochemi Photobiology 24, 587-593.

Berger D. S. (1982), A Climatology of Sunburning Ultraviolet Radiation, Photochemistry and Photobiology Vol. 35, pp 187 to 192, 1982.

Brewer Ozone Spectrophotometer Maintenance Manual (1985) MM-BA-C05, Feb.22, 1985, SCI-TEC Instr. Inc. 1526 Fletcher Rd, Saskatoon, Sask, CANADA, S7M 5M1.

Büttner K. (1969), The Effects of Natural Sunlight on Human Skin, pp. 237-249 in The Biological Effects of Ultraviolet Radiation, ed. Urbach F., Pergamon Press, 1969.

CIAP 5 (1975), Impacts of Climatic Change on the Biosphere. Climatic Impact Assessment Program, CIAP Monograph 5, U.S. Dept of Transportation, 1975.

Doda D.D. and Green A.E.S. (1981) Surface reflection measurements in the UV from an airborne platform, Part 2. Appl. Optics 1981, 20, pp 636-642.

Heath D.F. and Thekaekara (1977), The Solar Spectrum Between 1200 and 3000 Å pp 193-212 in The Solar Output and Its Variation, Edt by O.R. White, Colorado Ass. Univ. Press, Boulder.

ISES (1984), Glossary of terms used in solar energy, Solar Energy Vol. 33, No. 1, pp 97-114, 1984.

Kerr J. B. et al (1981), Measurements of Ozone with the Brewer ozone spectrophotometer, Proceedings of the Quadrennial International Ozone Symposium, Boulder, Colorado, April, 1981.

Kvifte et.al (1983), Spectral Distribution of Solar Radiation in the Nordic Countries, Jour. of Clim. and Appl. Meteor., Vol.22, No.1, Jan.1983.

Lala D. and Sjöström Ch. (1984), Solstrålning mot fasad och takmaterial, ny metod att mäta UV-strålning, Bygg och Teknik 4, 1984.

Latimer J. R. (1972), Radiation Measurement, IFGYL, Technical Manual Series No.2, Information Canada, Ottawa.

Liedquist L. and Wener G. (1984) Noggrannhet och felfaktorer vid optiska strålningsmätningar, del 2. Ultraviolet strålning från solarier och sollampor, Teknisk Rapport SP-RAPP 1984:14,, ISSN 0280-2503.

London and Bojkov (1963), The distribution of total ozone in the Northern hemisphere, Beitrige Phys Atmosphäre 36, 254-263.

Nicodemus F.E. (1981), Self-Study Manual on Optical Radiation Measurements, U.S. Dept of Commerce, Washington, D.C. 204 02.

Paltridge G. W. and Barton I. J. (1978), Erythmal Ultraviolet Radiation Distribution over Australia - the Calculations, Detailed Results and Input Data, CSIRO Austr. Div. Atmos. Phys., Tech. Pap. No. 33.

Saunders R. D. and Koskowski H. J. (1978), Accurate Solar Spectroradiometry in the UV-B. Optical Radiation News, No. 24, Apr 1978.

Sliney D. H. (1972), The Merits of an Envelope Action Spectrum for Ultraviolet Radiation Exposure Criteria, American Industrial Hygiene Association, 1972.

Wester U. (1981), A Simple Formulae Approximation of the ACGIH Curve of Relative Spectral Effectiveness of Actinic UV. Internal Report RI 1981-02, Radiofysiska institutionen, Karolinska Institutet, Box 60204, S-104 01, Stockholm, Sweden, 1981.

Wester U. (1983), Solar Ultraviolet Radiation - A Method for Measuring and Monitoring, Internal Report RI 1983-02.

Wester U. (1984), Erythmal Efficiency of Ultraviolet Radiation from the Sun and from Sunlamps Calculated on the basis of Measured Spectral Data. Internal Report RI 1984-05.

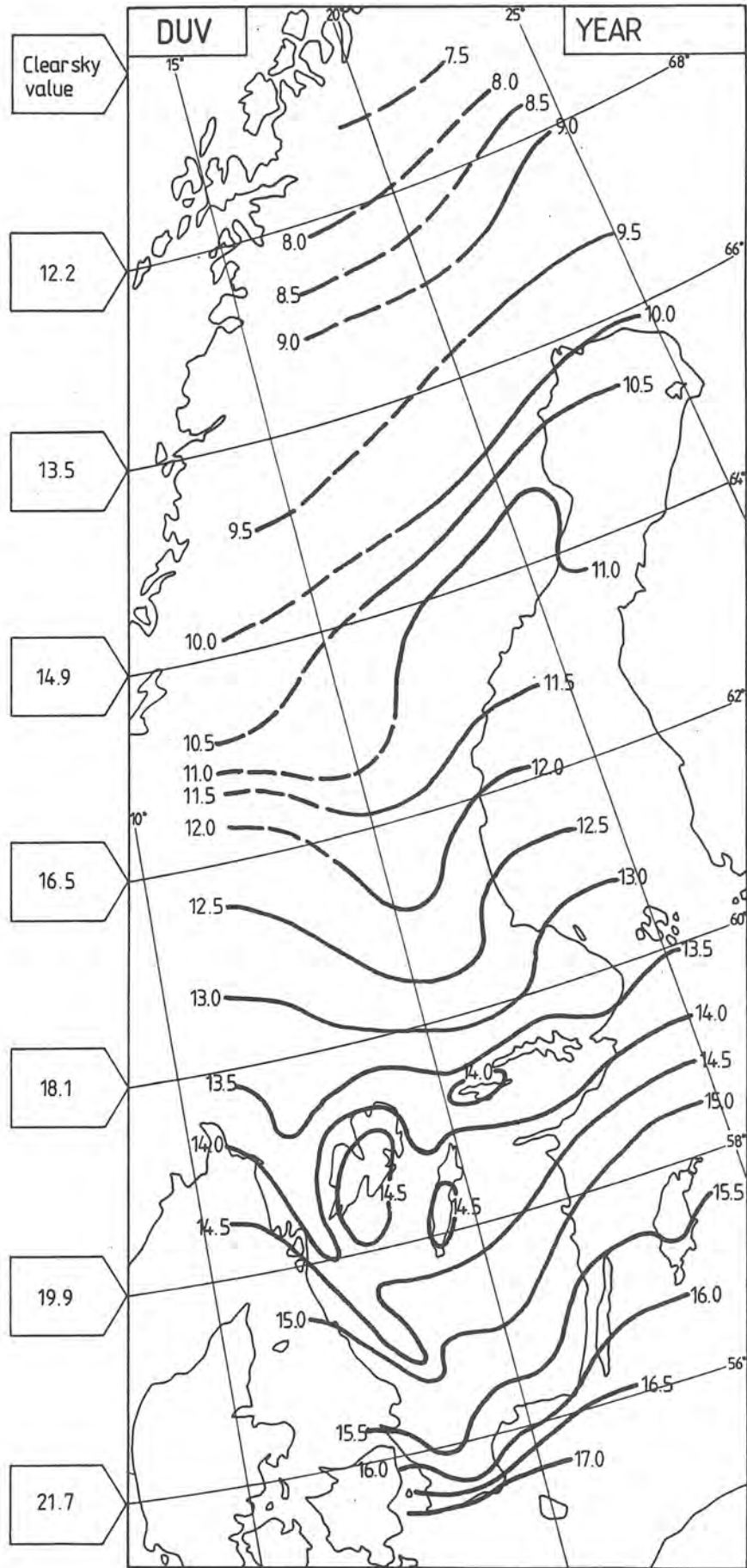
APPENDIX

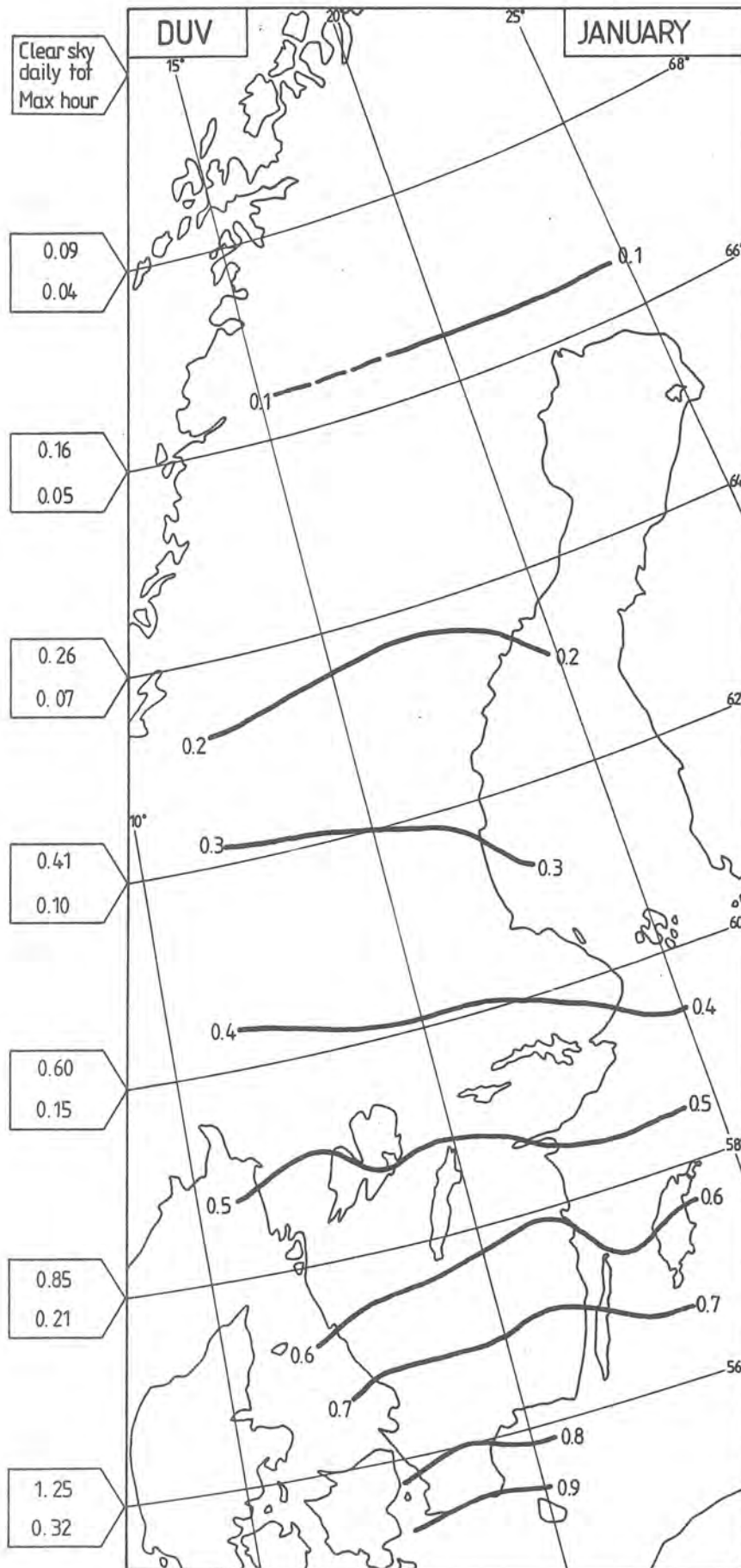
Maps of the average distribution of DUV on a horizontal surface in Sweden.

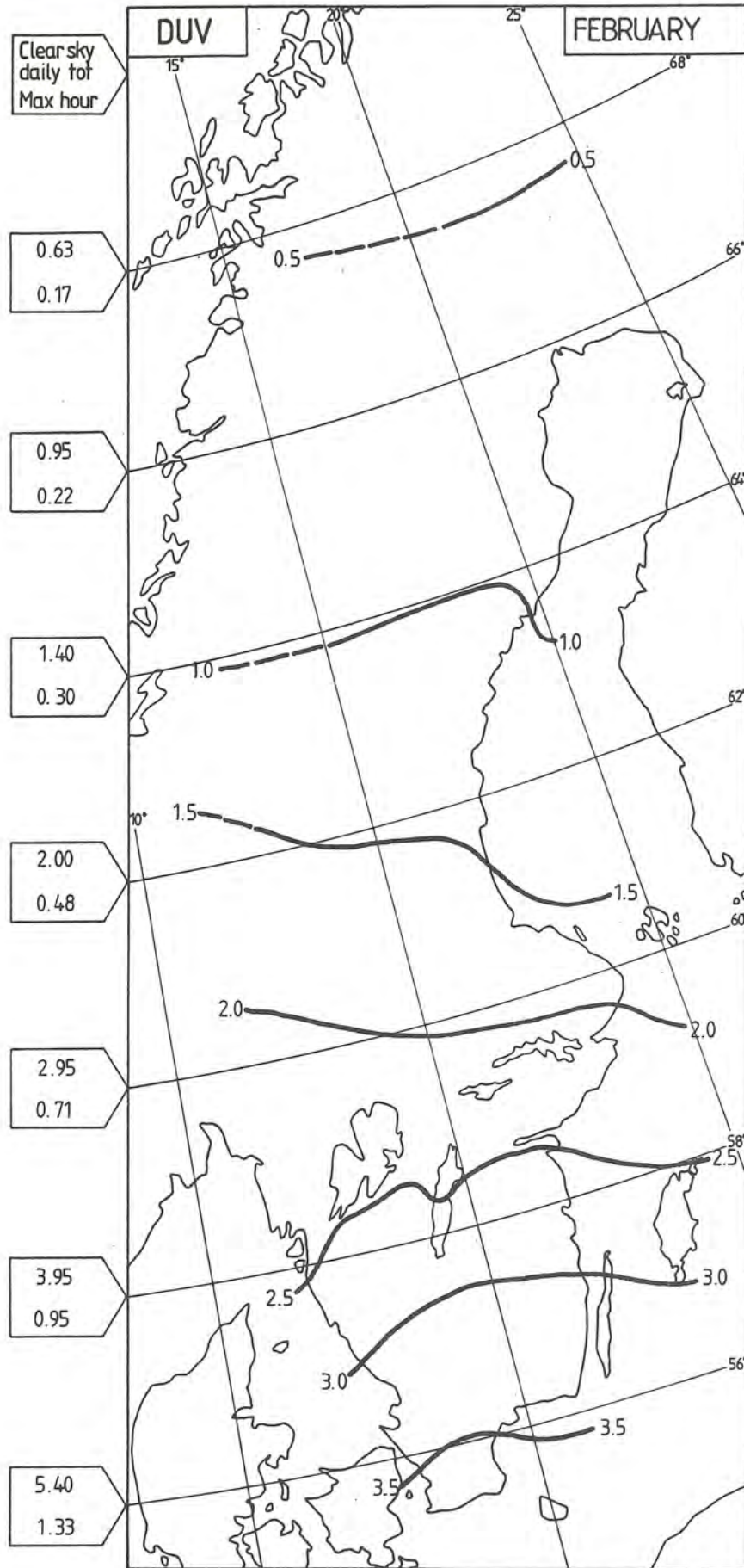
In squares to the left of every second degree of latitude clear day values for the midpoint of each month can be found. The upper figure gives the daily total and the lower one corresponds to the hourly value close to noon. The values given on the map of the year show the irradiation that could be if there was no clouds.

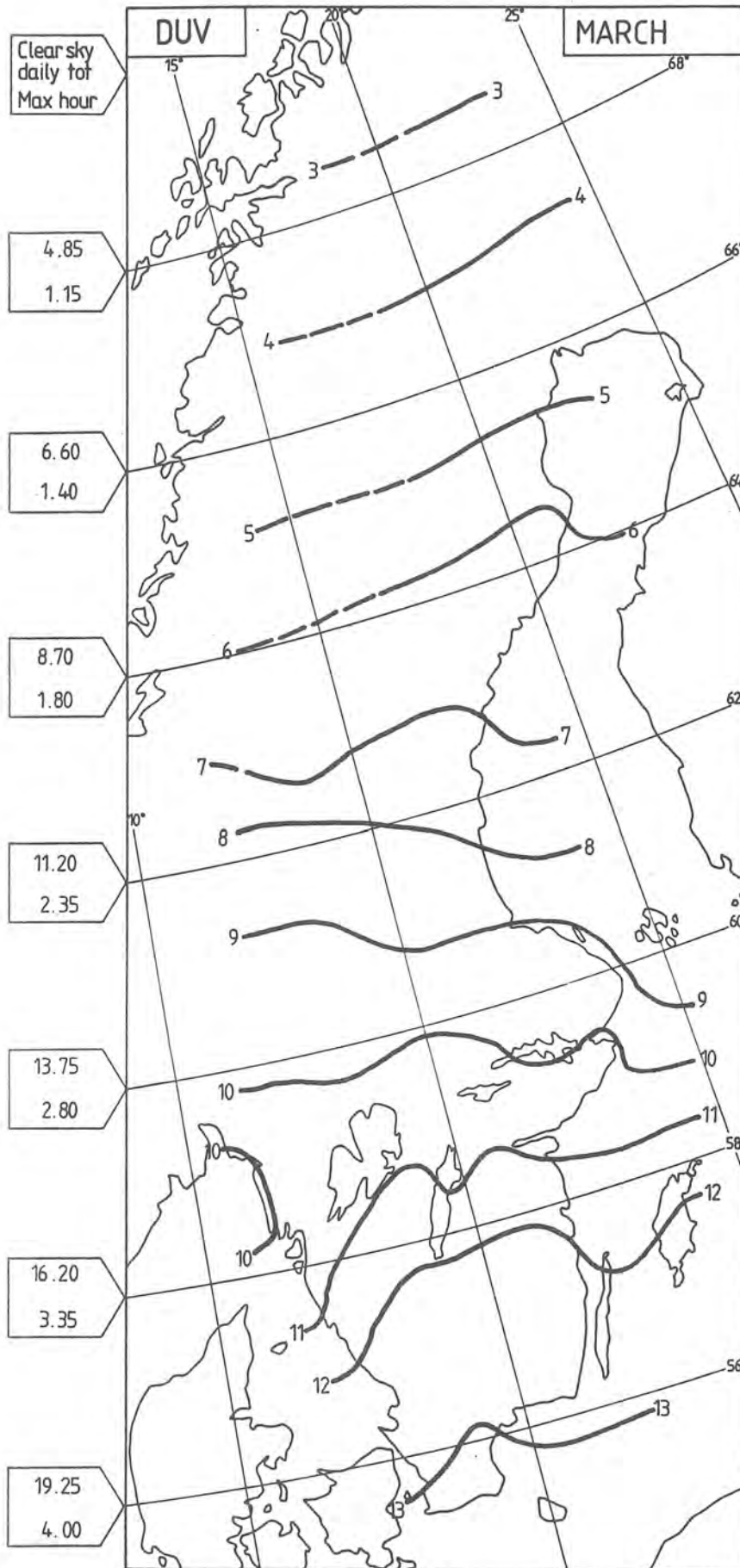
YEAR: Unit: Whm^{-2}
Square: a year with no clouds

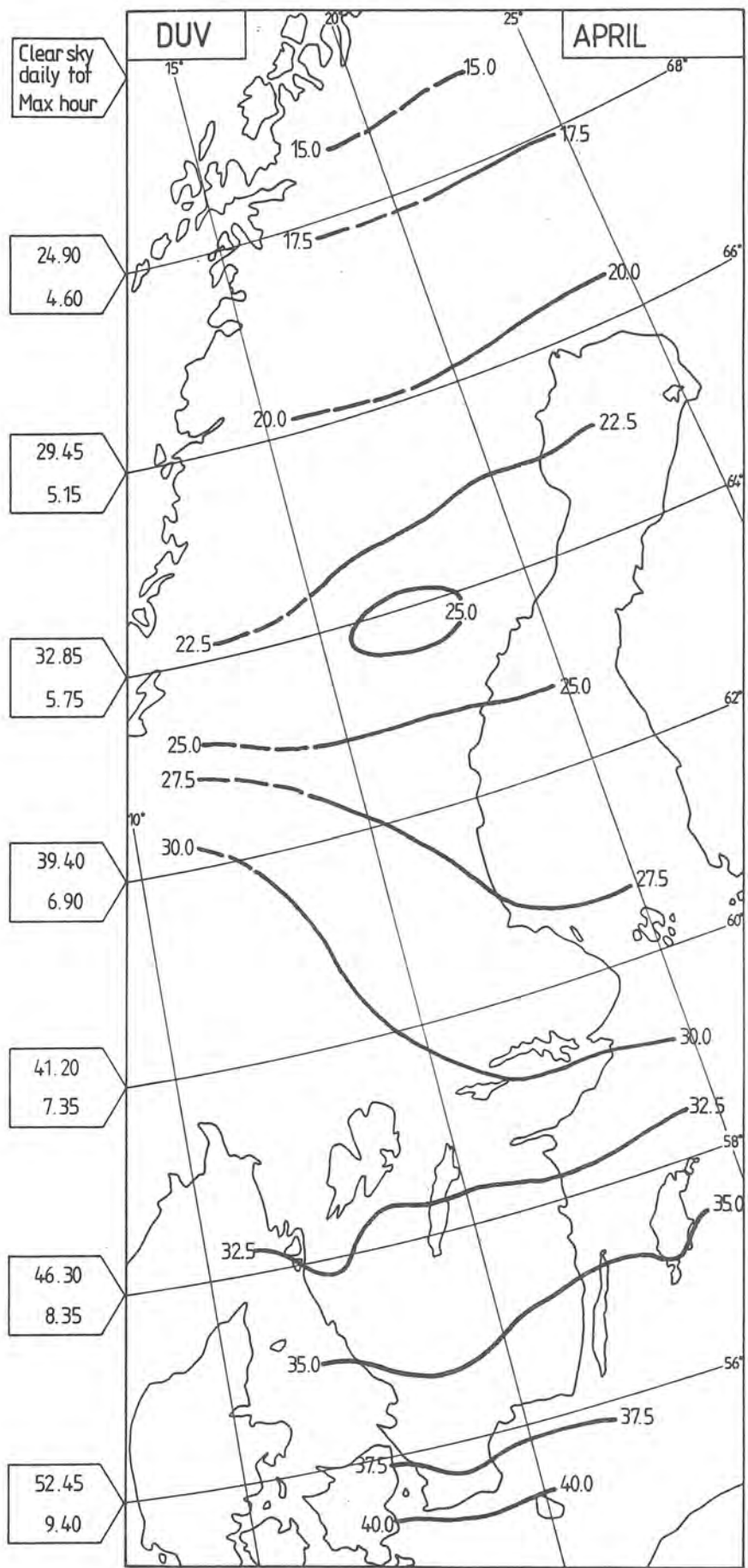
MONTHS: Unit: $\text{mWhm}^{-2} / \text{day}$
Square: an average clear day and
the maximum hourly value of that day

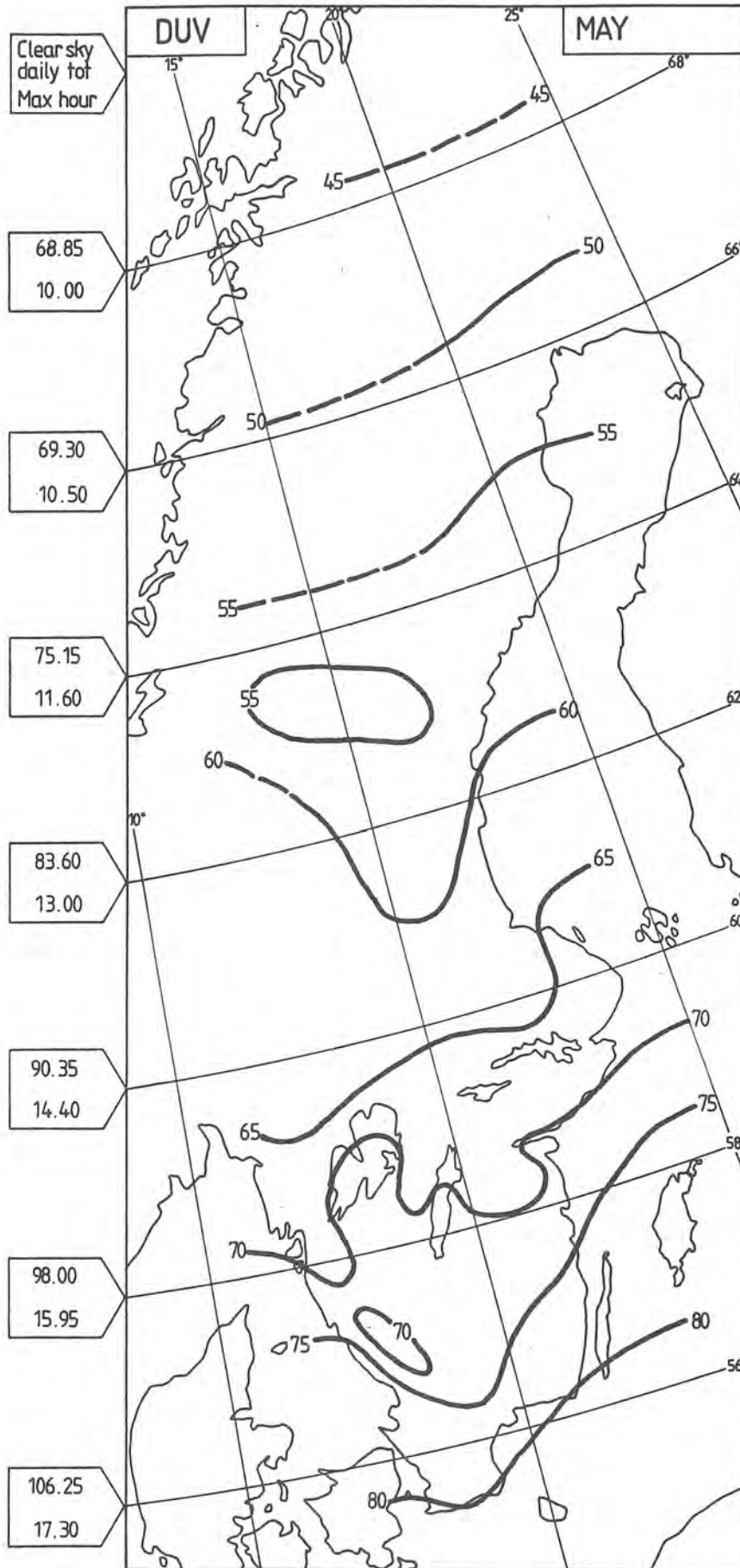


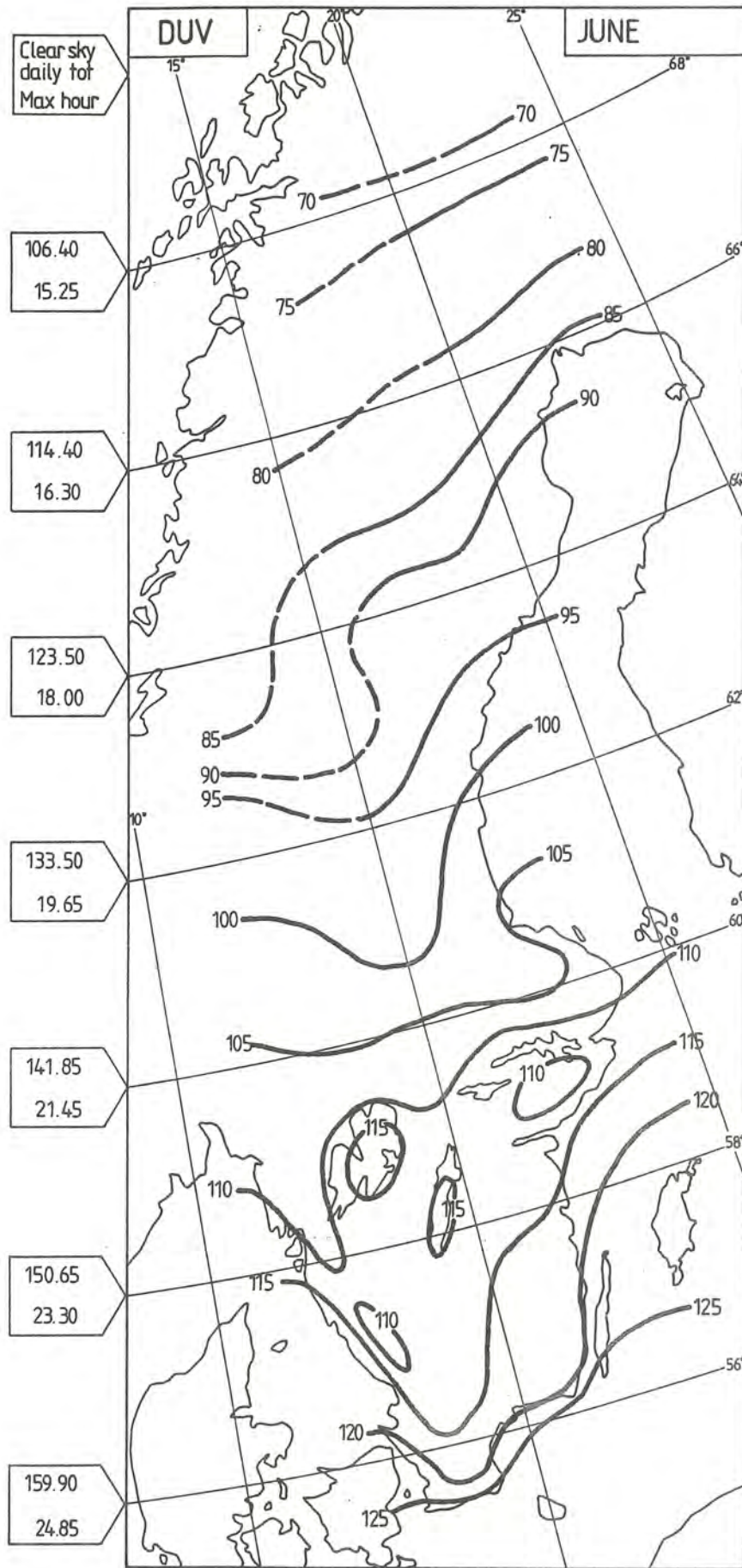


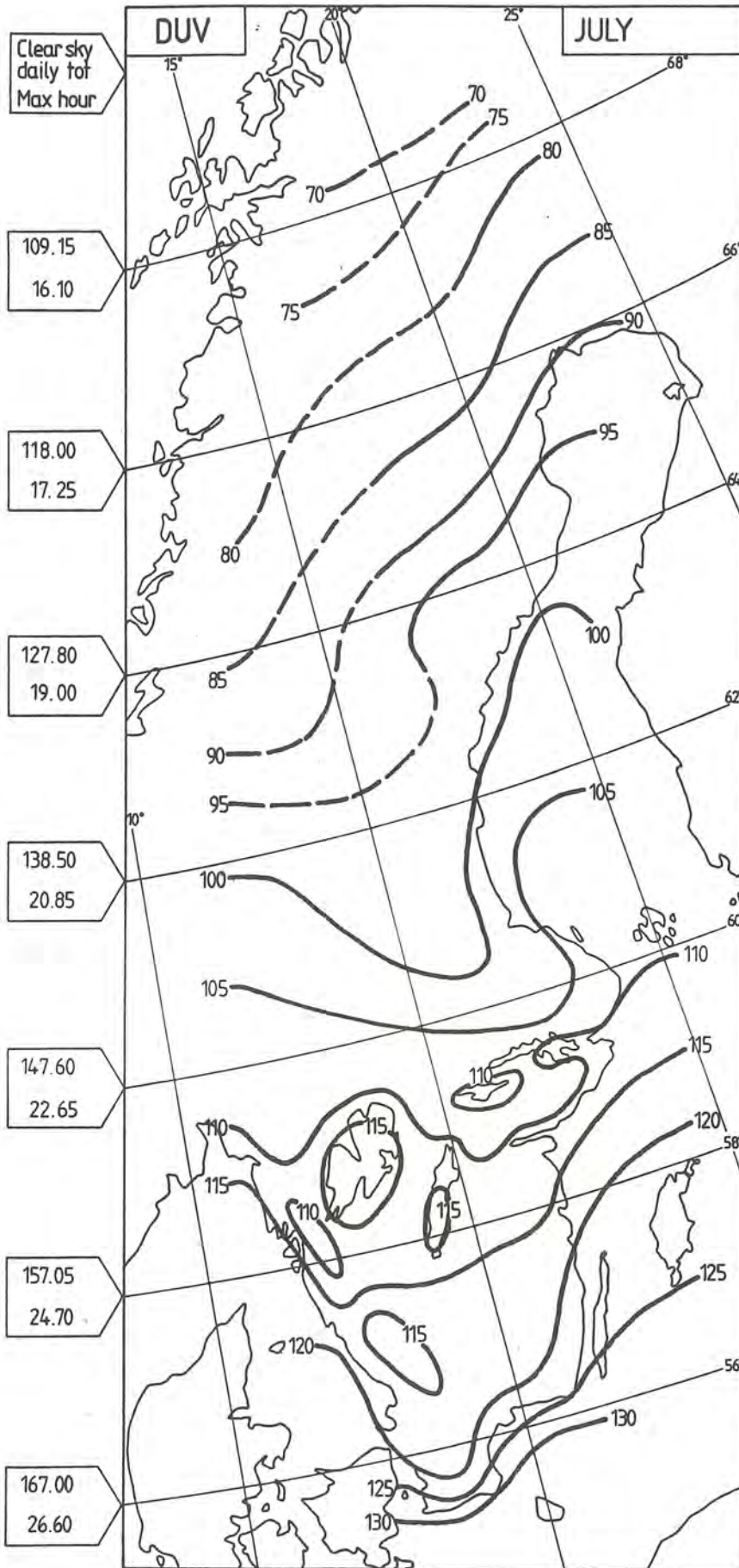


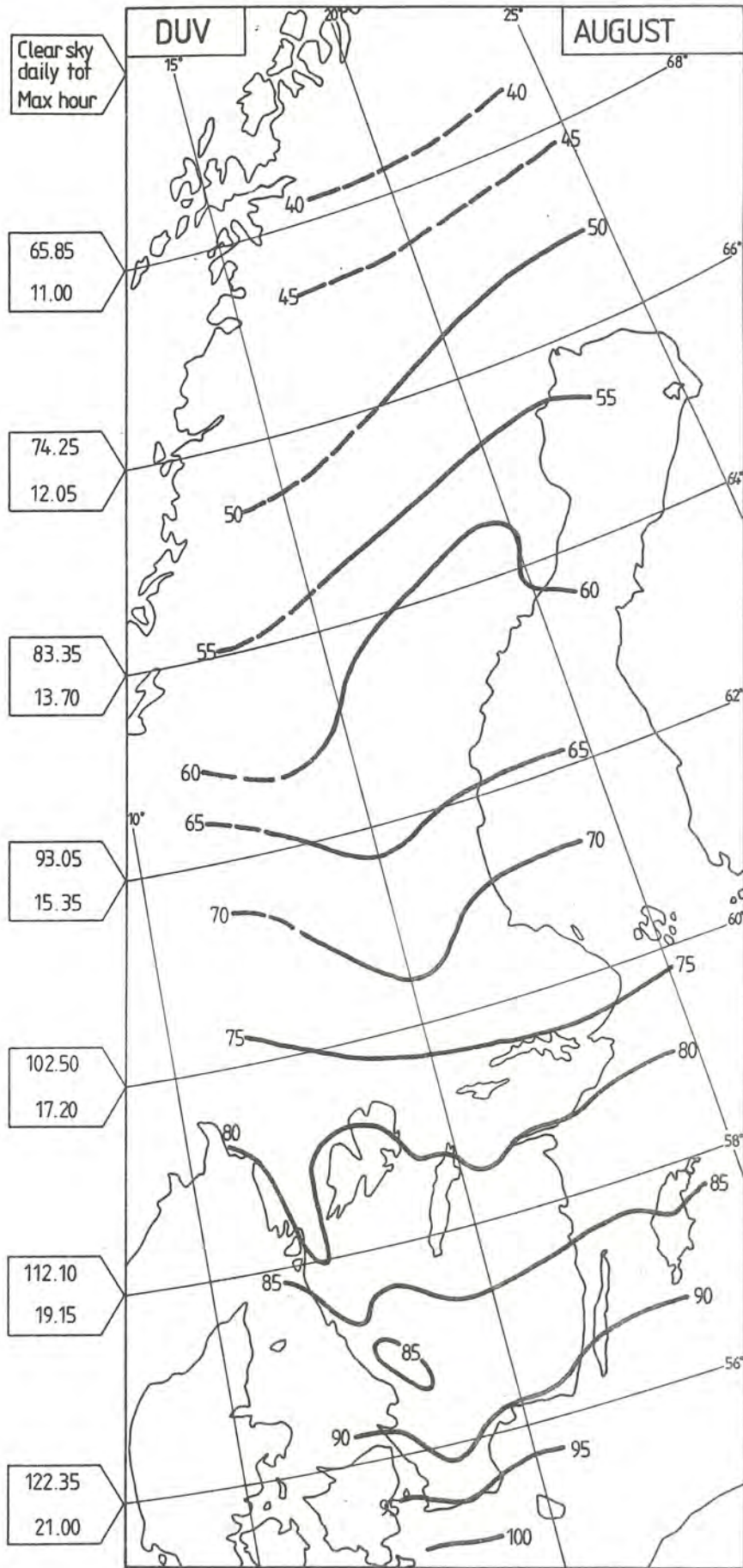


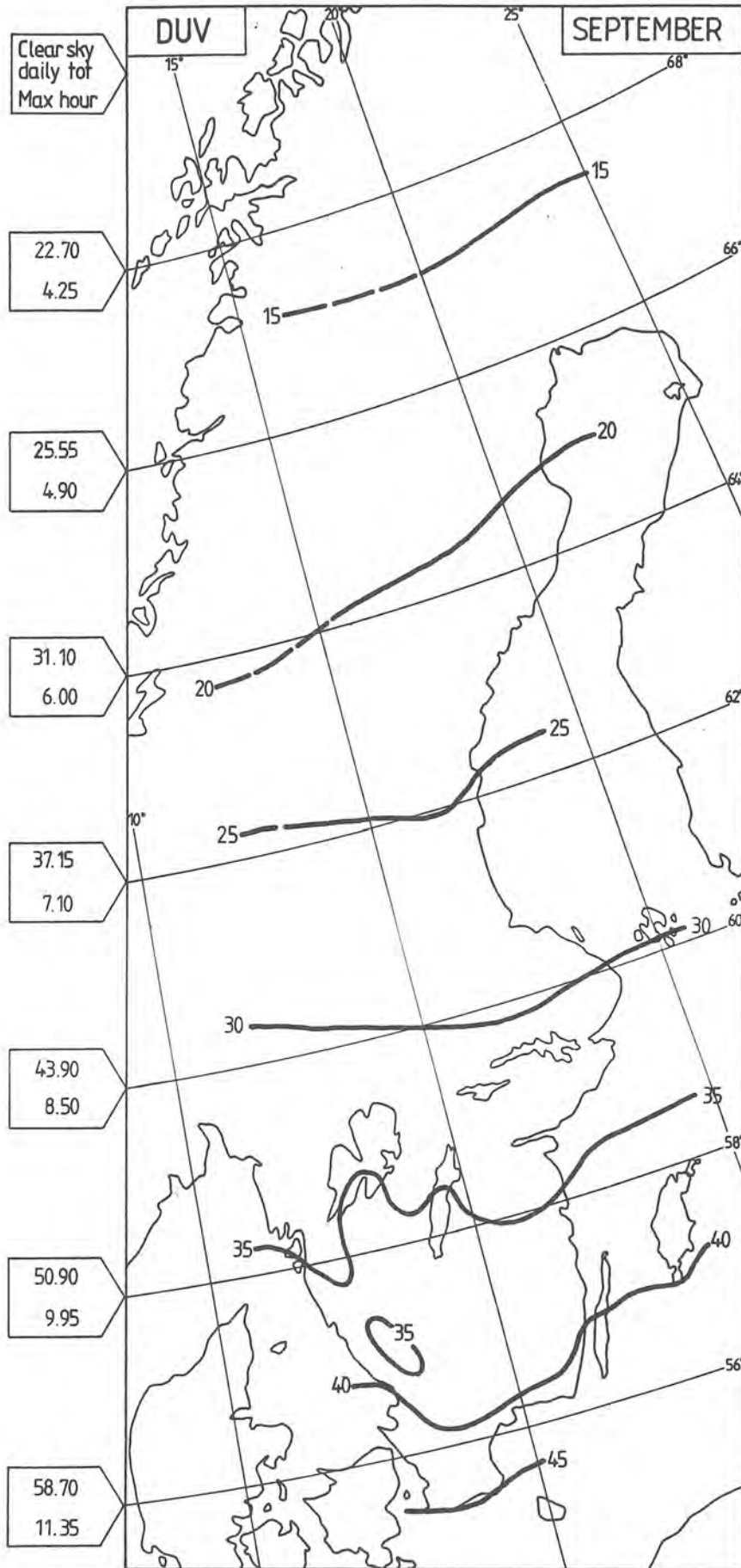


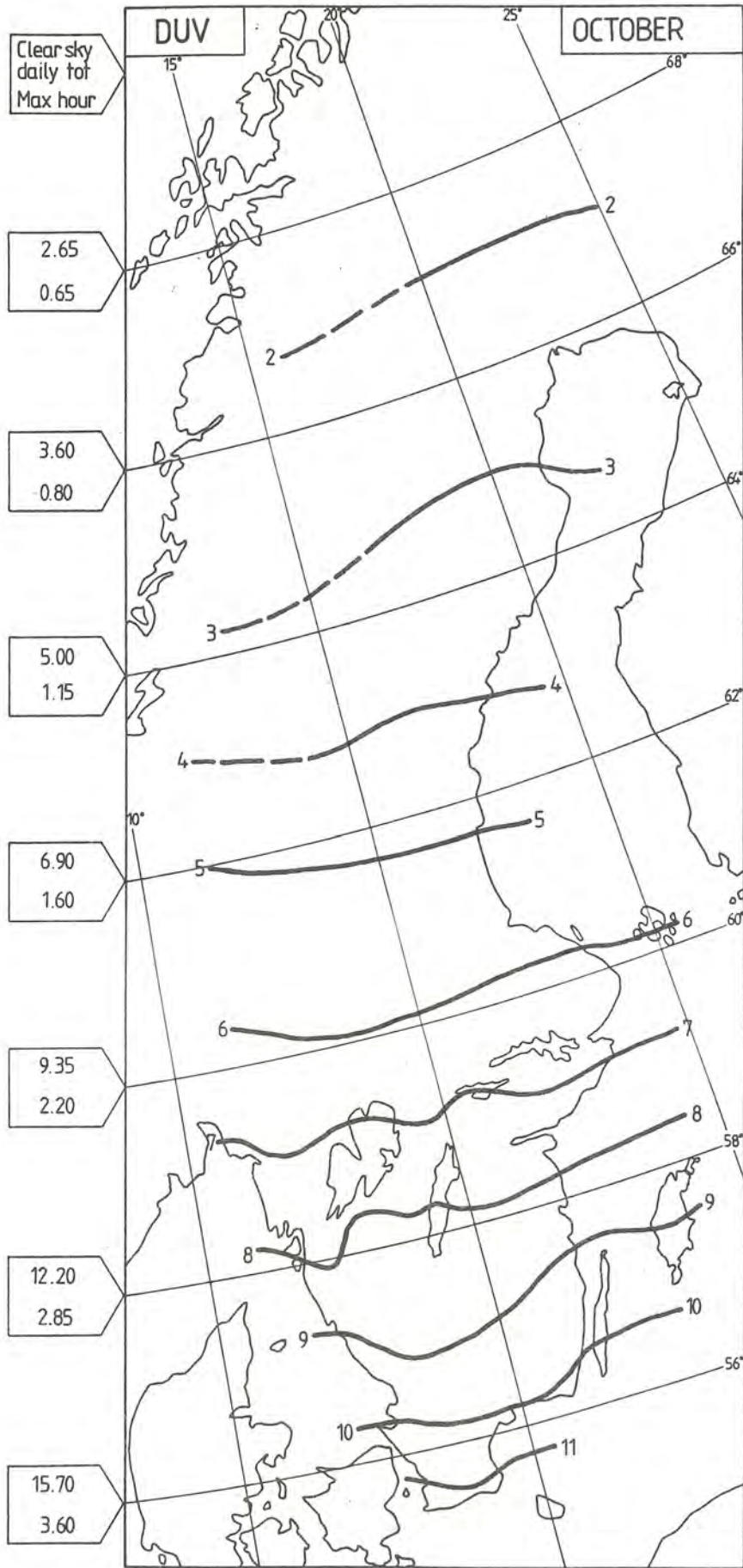


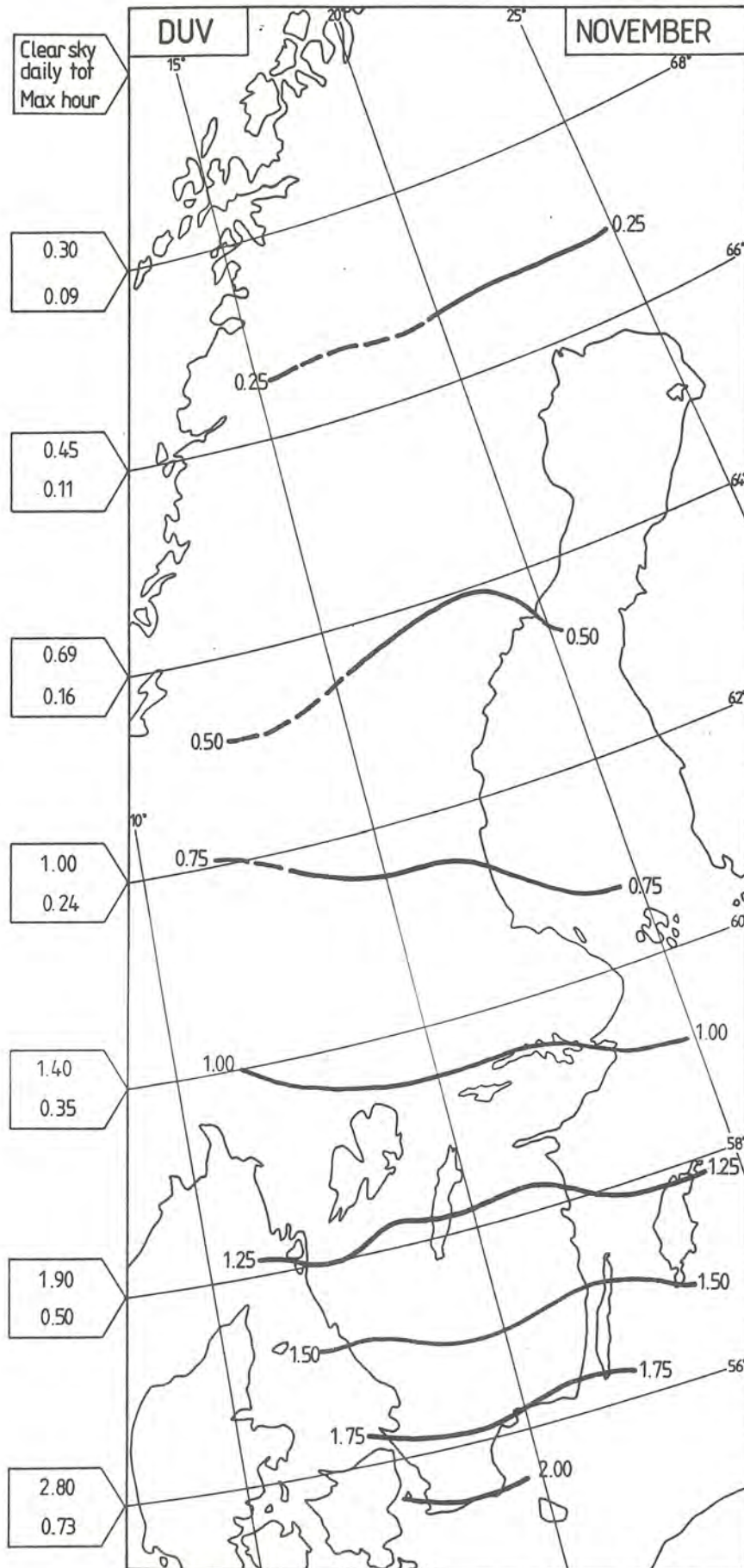


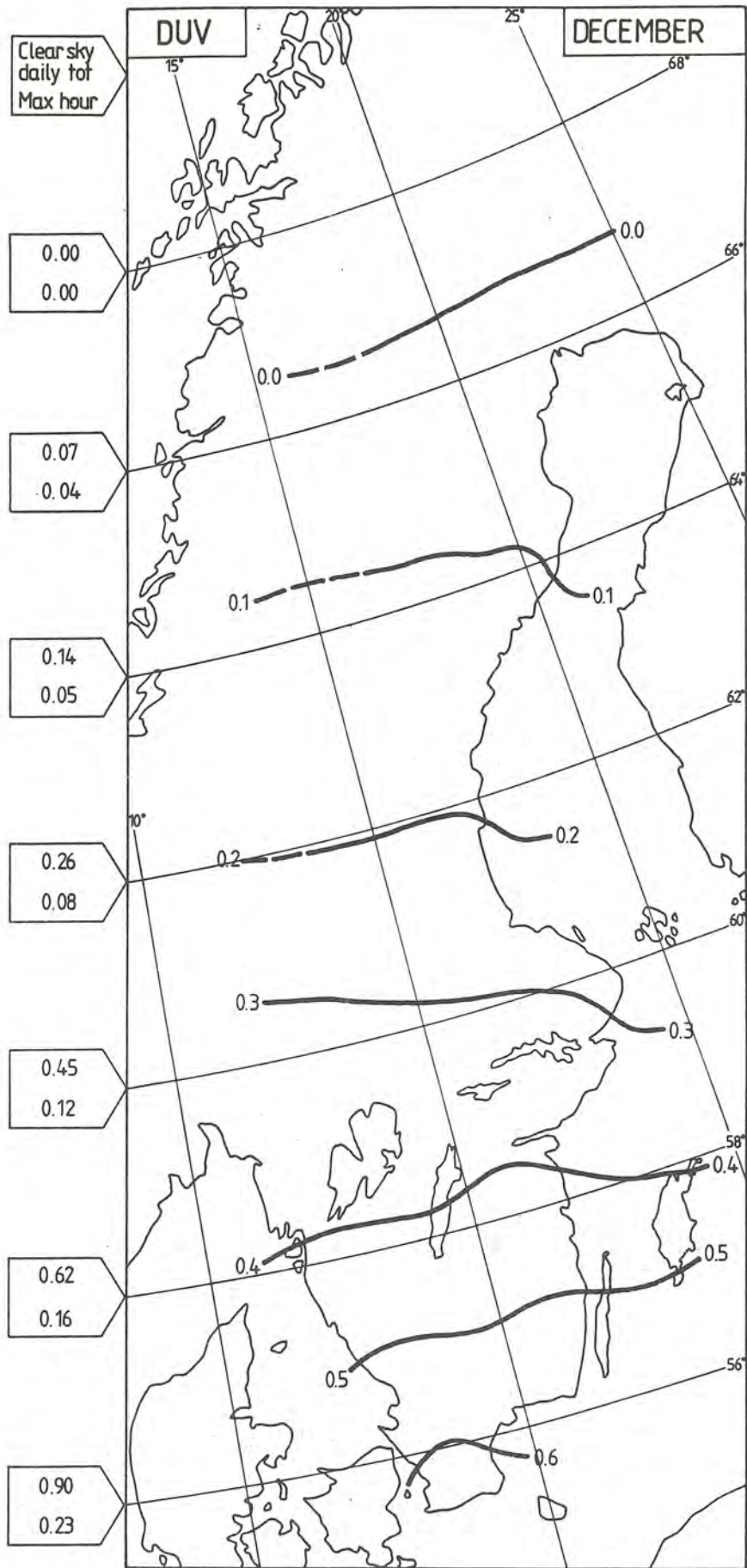












SMHI Rapporter, METEOROLOGI OCH KLIMATOLOGI (RMK)

- Nr 1 Thompson, T, Udin, I, and Omstedt, A
Sea surface temperatures in waters surrounding Sweden
Stockholm 1974
- Nr 2 Bodin, S
Development on an unsteady atmospheric boundary layer model.
Stockholm 1974
- Nr 3 Moen, L
A multi-level quasi-geostrophic model for short range weather
predictions
Norrköping 1975
- Nr 4 Holmström, I
Optimization of atmospheric models
Norrköping 1976
- Nr 5 Collins, W G
A parameterization model for calculation of vertical fluxes
of momentum due to terrain induced gravity waves
Norrköping 1976
- Nr 6 Nyberg, A
On transport of sulphur over the North Atlantic
Norrköping 1976
- Nr 7 Lundqvist, J-E, and Udin, I
Ice accretion on ships with special emphasis on Baltic
conditions
Norrköping 1977
- Nr 8 Eriksson, B
Den dagliga och årliga variationen av temperatur, fuktighet
och vindhastighet vid några orter i Sverige
Norrköping 1977
- Nr 9 Holmström, I, and Stokes, J
Statistical forecasting of sea level changes in the Baltic
Norrköping 1978
- Nr 10 Omstedt, A, and Sahlberg, J
Some results from a joint Swedish-Finnish sea ice experi-
ment, March, 1977
Norrköping 1978
- Nr 11 Haag, T
Byggnadsindustrins väderberoende, seminarieuppsats i före-
tags ekonomi, B-nivå
Norrköping 1978
- Nr 12 Eriksson, B
Vegetationsperioden i Sverige beräknad från temperatur-
observationer
Norrköping 1978
- Nr 13 Bodin, S
En numerisk prognosmodell för det atmosfäriska gränsskiktet
grundad på den turbulenta energiekvationen
Norrköping 1979
- Nr 14 Eriksson, B
Temperaturfluktuationer under senaste 100 åren
Norrköping 1979
- Nr 15 Udin, I, och Mattiasson, I
Havis- och snöinformation ur datorbearbetade satellitdata
- en modellstudie
Norrköping 1979
- Nr 16 Eriksson, B
Statistisk analys av nederbördsdata. Del I. Arealnederbörd
Norrköping 1979
- Nr 17 Eriksson, B
Statistisk analys av nederbördsdata. Del II. Frekvensanalys
av månadsnederbörd
Norrköping 1980
- Nr 18 Eriksson, B
Årsmedelvärden (1931-60) av nederbörd, avdunstning och
avrinning
Norrköping 1980
- Nr 19 Omstedt, A
A sensitivity analysis of steady, free floating ice
Norrköping 1980
- Nr 20 Persson, C och Omstedt, G
En modell för beräkning av luftföroreningars spridning och
deposition på mesoskala
Norrköping 1980
- Nr 21 Jansson, D
Studier av temperaturinversioner och vertikal vindskjvning
vid Sundaöarna-Härnösands flygplats
Norrköping 1980
- Nr 22 Sahlberg, J and Törnevik, H
A study of large scale cooling in the Bay of Bothnia
Norrköping 1980
- Nr 23 Ericson, K and Hårsmar, P-O
Boundary layer measurements at Klockrike. Oct. 1977
Norrköping 1980
- Nr 24 Bringfelt, B
A comparison of forest evapotranspiration determined by some
independent methods
Norrköping 1980
- Nr 25 Bodin, S and Fredriksson, U
Uncertainty in wind forecasting for wind power networks
Norrköping 1980
- Nr 26 Eriksson, B
Gräddagsstatistik för Sverige
Norrköping 1980
- Nr 27 Eriksson, B
Statistisk analys av nederbördsdata. Del III. 200-åriga
nederbördsserier
Norrköping 1981
- Nr 28 Eriksson, B
Den "potentiella" evapotranspirationen i Sverige
Norrköping 1981
- Nr 29 Pershagen, H
Maximianödjup i Sverige (perioden 1905-70)
Norrköping 1981
- Nr 30 Lönnqvist, O
Nederbördsstatistik med praktiska tillämpningar
(Precipitation statistics with practical applications)
Norrköping 1981
- Nr 31 Melgarejo, J W
Similarity theory and resistance laws for the atmospheric
boundary layer
Norrköping 1981
- Nr 32 Liljas, E
Analys av moln och nederbörd genom automatisk klassning av
AVHRR data
Norrköping 1981
- Nr 33 Ericson, K
Atmospheric Boundary layer Field Experiment in Sweden 1980,
GOTEX II, part I
Norrköping 1982
- Nr 34 Schoeffler, P
Dissipation, dispersion and stability of numerical schemes
for advection and diffusion
Norrköping 1982
- Nr 35 Undén, P
The Swedish Limited Area Model (LAM). Part A. Formulation
Norrköping 1982
- Nr 36 Bringfelt, B
A forest evapotranspiration model using synoptic data
Norrköping 1982
- Nr 37 Omstedt, G
Spridning av luftförorening från skorsten i konvektiva
gränsskikt
Norrköping 1982
- Nr 38 Törnevik, H
An aerobiological model for operational forecasts of pollen
concentration in th air
Norrköping 1982
- Nr 39 Eriksson, B
Data rörande Sveriges temperaturklimat
Norrköping 1982
- Nr 40 Omstedt, G
An operational air pollution model using routine meteorologi-
cal data
Norrköping 1984
- Nr 41 Christer Persson and Lennart Funkquist
Local scale plume model for nitrogen oxides.
Model description.
Norrköping 1984
- Nr 42 Stefan Gollvik
Estimation of orographic precipitation by dynamical
interpretation of synoptic model data.
Norrköping 1984
- Nr 43 Olov Lönnqvist
Congression - A fast regression technique with a great number
of functions of all predictors.
Norrköping 1984
- Nr 44 Sten Laurin
Population exposure to SO₂ and NO_x from different sources in
Stockholm.
Norrköping 1984
- Nr 45 Jan Svensson
Remote sensing of atmospheric temperature profiles by TIROS
Operational Vertical Sounder.
Norrköping 1985
- Nr 46 Bertil Eriksson
Nederbörds- och humiditetsklimat i Sverige under vegetations-
perioden
Norrköping 1986
- Nr 47 Roger Taesler
Köldperioder av olika längd och förekomst
Norrköping 1986
- Nr 48 Wu Zengmao
Numerical study of lake-land breeze over Lake Vättern
Sweden
Norrköping 1986
- Nr 49 Wu Zengmao
Numerical analysis of initialization procedure in a two-
dimensional lake breeze model
Norrköping 1986
- Nr 50 Persson, Christer
Local scale plume model for nitrogen oxides. Verification.
Norrköping 1986
- Nr 51 Melgarejo, José W.
An analytical model of the boundary layer above sloping
terrain with an application to observations in Antarctica
Norrköping 1986
- Nr 52 Bringfelt, B.
Test of a forest evapotranspiration model
Norrköping 1986



Swedish meteorological and hydrological institute
S-60176 Norrköping, Sweden. Tel. +4611158000. Telex 64400 smhi s.